SQT

DOE/NASA/0817-1
NASA CR-165168
Draper Report R-1489

DEVELOPMENT OF A DUAL-FIELD HETEROPOLAR POWER CONVERTER

David B. Eisenhaure
Bruce G. Johnson
Tim E. Bliamptis
Emery St. George

August 1981

Prepared for
NATIONAL AERONAUTICS AND SPACE ADMINISTRATION
Lewis Research Center
Under Contract NAS3-20817

for
U.S. DEPARTMENT OF ENERGY
Conservation and Renewable Energy
Office of Vehicle and Engine R&D

TECHNICAL REPORT STANDARD TITLE PAGE

1. Report No.	2. Government Accession No.	3. Recipient's Catalog No.
NASA CR-165168		

4. Title and Subtitle	5. Report Date
DEVELOPMENT OF A DUAL-FIELD HETEROPOLAR POWER CONVERTER	August 1981
	6. Performing Organization Code

7. Author(s)	8. Performing Organization Report No.
D.Eisenhaure, B.Johnson, T.Bliamptis, E.St.George	R-1489

9. Performing Organization Name and Address	10. Work Unit No.
Charles Stark Draper Laboratory Inc. 555 Technology Square Cambridge, Mass. 02139	11. Contract or Grant No. NAS3-20817
	13. Type of Report and Period Covered Contractor Report
12. Sponsoring Agency Name and Address U.S. Department of Energy Conservation and Renewable Energy Office of Vehicle and Engine R&D Washington, D.C. 20585	14. Sponsoring Agency Code DOE/NASA 0817-1

15. Supplementary Notes
Final Report. Prepared under Interagency Agreement DE-A101-77CS1044
Project Manager, E. McBrien, Electric Vehicle Components Section,
NASA Lewis Research Center, Cleveland, Ohio 44135

16. Abstract

This report describes the design and test of a 400 watt, dual phase, dual rotor, field modulated inductor alternator. The system is designed for use as a flywheel to AC utility line or flywheel to DC bus (electric vehicle) power converter. The machine is unique in that it uses dual rotors and separately controlled fields to produce output current and voltage which are in phase with each other. Having the voltage and current in phase allows the power electronics to be madeof simple low cost components.

Based on analytical predictions and experimental results, development of a complete 22 kilowatt (30 Hp) power conversion system is recommended. This system would include power electronics and controls and would replace the inductor alternator with an improved electromagnetic conversion system.

17. Key Words Suggested by Author	18. Distribution Statement
Field Modulation; Power Conversion; Variable Speed to Constant Frequency; Frequency Converter; Inductor Alternator; Flywheel Electric Vehicle	Unclassified - unlimited STAR Category 33 DOE Category UC-96

19. Security Classif. (of this report)	20. Security Classif. (of this page)	21. No. of Pages	22. Price
Unclassified.	Unclassified.		

DOE/NASA/0817-1
NASA CR-165168
Draper Report R-1489

DEVELOPMENT OF A DUAL-FIELD HETEROPOLAR POWER CONVERTER

David B. Eisenhaure
Bruce G. Johnson
Tim E. Bliamptis
Emery St. George

August 1981

Prepared for
NATIONAL AERONAUTICS AND SPACE ADMINISTRATION
Lewis Research Center
Under Contract NAS3-20817

for
U.S. DEPARTMENT OF ENERGY
Conservation and Renewable Energy
Office of Vehicle and Engine R&D
Washington, D.C. 20585
Under Interagency Agreement DE-AI01-77CS1044

TABLE OF CONTENTS

1. SUMMARY

This report describes the design and test of a 400 watt inductor alternator. The inductor alternator was designed and tested by the Charles Stark Draper Laboratory, Inc. (CSDL) under contract to the National Aeronautics and Space Administration, Lewis Research Center (NASA/LeRC). This research advances the development of flywheel to AC utility line and flywheel to DC bus (electric vehicle) power conversion systems.

In its final configuration, the inductor alternator consists of a dual phase, dual rotor, field modulated electromechanical system with associated power electronics, test bed, and controller. The use of a variable reluctance machine (inductor alternator) combined with field modulation allows the system to couple high and variable shaft speeds (5,000-10,000 rpm) with fixed frequency electrical networks. Also, with dual rotors and separately controlled fields, the output voltage and current are in phase with each other. This allows the power electronics to be made of simple, low cost components. With no filtering, output ripple of 6% was achieved over the 2 to 1 speed range. These advantages are somewhat offset by the baseline system's relatively low power density and efficiency.

An analytical model of the inductor alternator was developed. The agreement between the model's predictions and experimental measurements is quite good. The model predicts that the efficiency could be raised by

increasing the winding volume. The use of higher shaft speeds and a less conservative design could increase the power density by a factor of 30.

Development of a complete 22 kilowatt (30 HP) power conversion system for electric vehicles is recommended. This system would include power electronics and controls and would replace the inductor alternator with an improved electromagnetic conversion system.

2. INTRODUCTION

2.1 BACKGROUND

A need exists for systems which store electrical utility power during off-peak hours. Flywheel energy storage is a promising system that can meet this need. Flywheels are reliable, long lasting, and inexpensive and can potentially store energy efficiently at high energy densities.

In an effort to improve performance at the interface between the flywheel and the utility grid, The Charles Stark Draper Laboratory, Inc. (CSDL) studied the conceptual design and development of advanced suspension and energy conversion subsystems. These studies were sponsored by the National Science Foundation, NSF Grant AER75-18813, and were completed in November 1977 (1). Initially directed toward utility load leveling, the studies were later expanded toward applications in electric vehicles, mass transit, and solar or wind energy generation systems.

The function of the flywheel energy storage system in a utility grid is leveling the electrical load in the generation/distribution system. Thus the flywheel will store energy when electrical demand is less than generation and provide energy when demand is greater than generation. To reduce the reactive power in the grid, the system should also independently provide power factor correction. With these system objectives

in view, a detailed set of desired characteristics for an energy conversion system which interfaces a flywheel shaft and an AC line was formulated at Draper. The system should:

1. Handle independently-controlled amounts of real and reactive power (power factor correction).

2. Provide motor/generator operation in a single electromechanical unit.

3. Provide controlled output frequency, voltage and power from a variable speed shaft.

4. Provide stand-alone or grid-coupled capability.

5. Provide waveforms with low harmonic content after minimal filtering.

6. Provide high efficiency and high power density at low cost.

The different types of energy converters which can match the high, variable shaft speed (5,000-10,000 rpm) of a flywheel to a fixed frequency electrical grid are shown schematically in Figure 2-1. The suitability of these various conversion systems for flywheel applications was analyzed; the results are shown in Table 2-1, and are summarized below. Details of the analysis can be found in Reference (1).

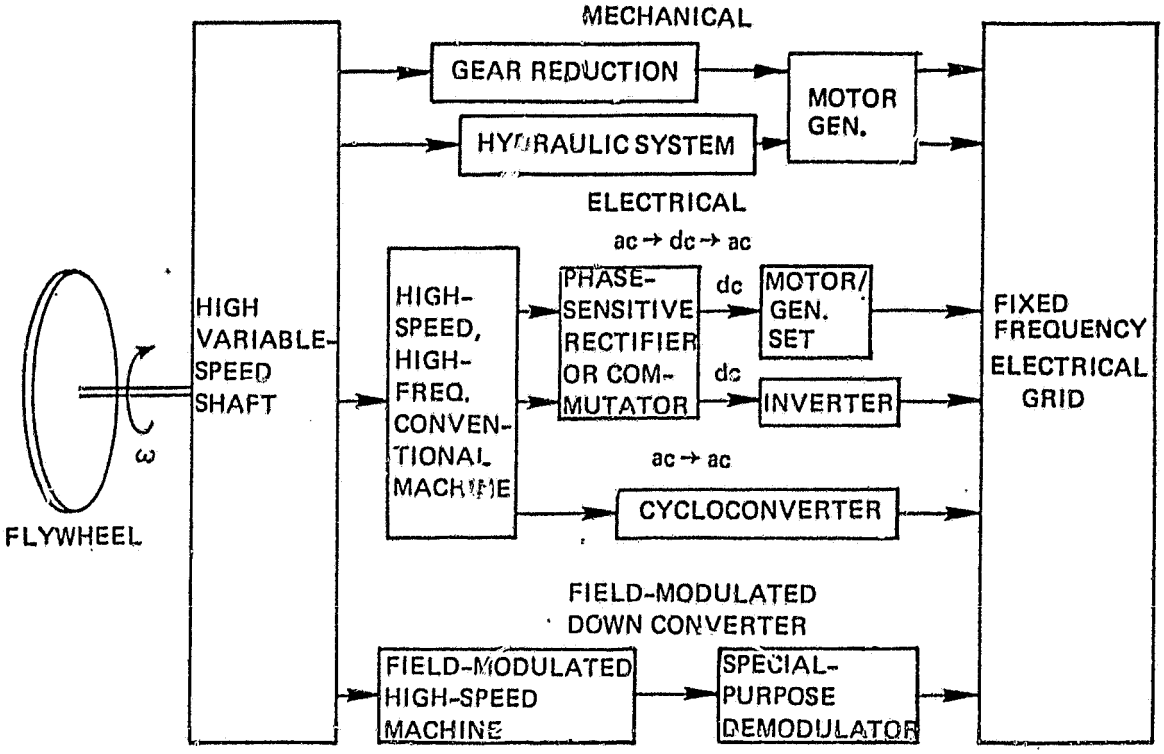

Figure 2.1. Possible Flywheel Energy Conversion Systems

All of the high efficiency, high power density conversion systems require some type of motor/generator which can operate at the flywheel shaft speed, a high shaft speed being necessary so that the flywheel can be light and compact. At these high speeds, motor/generators with brushes are undesirable, since the brushes are unreliable, high maintenance devices. All electrical connections to the rotor should therefore be

Table 2-1. Comparison of Frequency Down Systems

SYSTEM TYPE	SUITABILITY FOR FLYWHEEL APPLICATION
Mechanical:	
Speed reducers	Complex (especially for variable speed) Expensive High losses Large rotating machine (low speed)
Electrical:	
Multiple machines	Expensive, heavy; requires multiple rotating machines at full power level
AC-DC-AC	Inverter stage is expensive and unreliable Large EMI generation Each phase of generator not continuously loaded
Cycloconverter	Poor waveform quality (filter required) Inefficient use of machine Large EMI generation Each phase of generator not continuously loaded
Conventional field modulated down converter	No intrinsic regeneration capability Difficulty handling reactive power waveform distortion
CSDL dual field modulation system	Meets flywheel conversion system desired characteristics Offers significant advantages over conventional approaches

made with either rotary transformers or separate exciters. Also, in these high speed applications, the high rotor stresses may prevent the use of a wound rotor motor/generator. Two alternatives to a wound rotor motor/generator are a permanent-magnet rotor or a variable reluctance (inductor alternator) motor/generator.

A permanent magnet motor/generator has two significant problems when used in this application. First, since the magnetic field is a constant, continuous losses are incurred in the stator iron even when the motor/generator is coasting. This problem can be eliminated by suspending the stator coils and rotating the back iron with the rotor. However, the elimination of this problem requires a complex, unconventional design. Second, since the generated voltage is proportional to speed and must equal the line voltage at minimum speed, the generated voltage will be at least twice the line voltage at maximum speed (twice minimum speed). Therefore, a variable voltage power converter stage is required. However, the permanent magnet machine generally has lower machine inductance than an equivalent wound rotor machine. Since this can be an advantage in semiconductor switched conversion systems, the permanent magnet machine remains a candidate, particularly when a DC output voltage is desired.

The variable reluctance machine (inductor alternator) is an attractive choice for the frequency down-converter. The problems of high speed brushes and wound rotor stress limits are avoided, since all the windings are on the stator. Also, field control, including modulation, is possible with the inductor alternator.

2.2 HISTORY OF THE PROGRAM

The National Areonautics and Space Administration, Lewis Research Center, (NASA/LeRC), contracted with CSDL to design, fabricate, and test a flywheel energy

conversion system based on the NSF sponsored studies. The NASA/LeRC program was originally aimed at developing a flywheel-to-AC line interface, with the system implemented as a bidirectional frequency converter. A dual rotor, field modulated inductor alternator was designed and partially fabricated.

At this point in the program, the system requirements were altered. A change in priorities at NASA/LeRC resulted in a contract modification calling for a shift in emphasis from the AC line interface to an electric vehicle (EV) application. In this application, the flywheel would be coupled with a battery; current surges would then be absorbed by the flywheel. To demonstrate the concept, the inductor alternator was therefore completed and tested as a DC-input/DC-output device. However, it was not anticipated that this particular CSDL inductor alternator would prove to be the optimum device for this application.

2.3 PROGRAM OVERVIEW

The system which was actually designed and built consists of a 400 watt breadboard conversion unit, which serves both as a proof of concept and as a foundation upon which further work can be built. The design was based on the original requirements for an AC line interface as listed in Section 2.4.1. Components based on this design were fabricated. Prior to assembly, the requirements were changed to the DC line interface, as given in Section 2.4.2. The machine was accordingly wound, assembled and tested to meet these latter requirements.

The conversion unit was tested as a flywheel to DC bus motor/generator. Power output, efficiency, and voltage ripple over a 5000-10000 RPM speed range were measured. Also, its use as a flywheel to AC line generator, as originally specified, was demonstrated. These experimental results were compared with predictions of the analytical models in order to validate these models. Recommendations of areas for further study were based on the test results and analytical models.

2.4 SYSTEM REQUIREMENTS

2.4.1 Original System Requirements

Contract No. NAS3-20817, dated July 13, 1978, from the National Aeronautics and Space Administration, Lewis Research Center, originally called for the design and test of a bidirectional power conversion system. Employing an inductor alternator and a solid-state switching network, the system was to operate from a 60 Hz line as a motor, and drive a 60 Hz load as a generator. The following system and component specifications were provided:

2.4.1.1 Original System Performance Specifications

Generator Mode

Input:

Speed Range	2:1 With Minimum Speed in the Range 5,000-10,000 RPM

Output:

Voltage Regulation	± 5% of Machine Rated Voltage
Frequency	60 Hz ± 2 Hz
Power Factor Range	0.7 - 1.0 Leading & Lagging
Continuous Power	400 Watts

Drive Mode

Input:

Voltage	± 10% of Machine Rated Voltage
Frequency	60 Hz ± 2 Hz
Power Factor Range	.07 - 1.0 Leading & Lagging
Continuous Power	400 Watts

Output:

Speed Range	2:1 With Minimum Speed in the Range 5,000-10,000RPM

2.4.1.2 Original System Component Specifications

Inductor-Alternator

Number of Phases	2
Number of Fields	2
Continuous Power Rating	400 Watts

Switching Network

Solid State Device Type	Thyristor
Thyristor Current Rating	Minimum of 125% of Machine Rated Current

2.4.2 Modified System Requirements

Contract modification No.1, dated August 1, 1979, replaced the original system performance and component specifications with the following:

2.4.2.1 Modified System Performance Specifications

Generator Mode

Input:

Speed Range	2:1 With Minimum Speed in the Range 5,000-10,000 RPM

Output:

DC Voltage Regulation	± 5% of Machine Rated Voltage
Continuous Power	400 Watts

Drive Mode

Input:

DC Voltage	± 10% of Machine Rated Voltage
Continuous Power	400 Watts

Output:	
Speed Range	2:1 With Minimum Speed in the Range 5,000-10,000 RPM

2.4.2.2 Modified System Component Specifications

Inductor-Alternator

Number of Phases	2
Number of Fields	2
Continuous Power Rating	400 Watts

3. INDUCTOR ALTERNATOR DESCRIPTION

3.1 VARIABLE RELUCTANCE

An inductor alternator is a synchronous motor/generator with both the field and input/output (i/o) windings on the stator. The basic features of the inductor alternator are shown in Figure 3.1. The field windings and input/output windings are coupled by a flux path which includes the rotor. To provide electromechanical power conversion, the rotor has distinct teeth, hence the desciption variable reluctance. Because there are no windings on the rotor, it is possible to use the inductor alternator at very high shaft speeds. The inductor alternator is a synchronous machine; it only converts power when a fixed relationship between shaft speed and electrical frequency is satisfied.

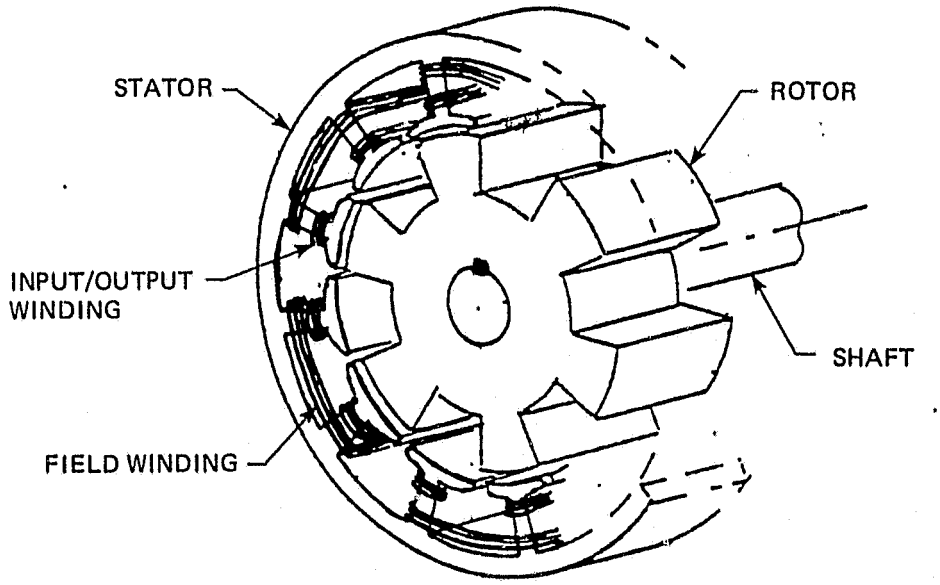

Figure 3.1. Single Rotor Inductor Alternator

When operating as a generator, a time varying magnetic flux is generated. As the rotor turns, the flux generated by the field windings is swept through different input/output coils producing a time varying flux in the input/output coils. A voltage, given by Faraday's Law, is induced in the i/o coils by the flux variation.

$$V = N\frac{d\Phi}{dt},$$

where V = induced voltage in the coil
Φ = magnetic flux through the coil
N = number of winding turns in the coil.

Each i/o coil sees the flux variation as a triangular waveform in time (Figure 3.2(a)). Due to Faraday's Law, the triangular flux waveform induces a square voltage waveform in the i/o windings (Figure 3.2(b)). The amplitude and period of the waveform is determined by rotor and stator dimensions, winding parameters, field current, and the shaft speed. The number of voltage waveform periods per rotor revolution is equal to the number of rotor teeth. Therefore, the frequency of the voltage waveform (in Hertz) is the shaft angular velocity (in revolutions per second) multiplied by the number of rotor teeth. Since an inductor alternator is a synchronous motor/generator, it only converts average power when this relationship between shaft angular velocity and generated electrical frequency is satisfied.

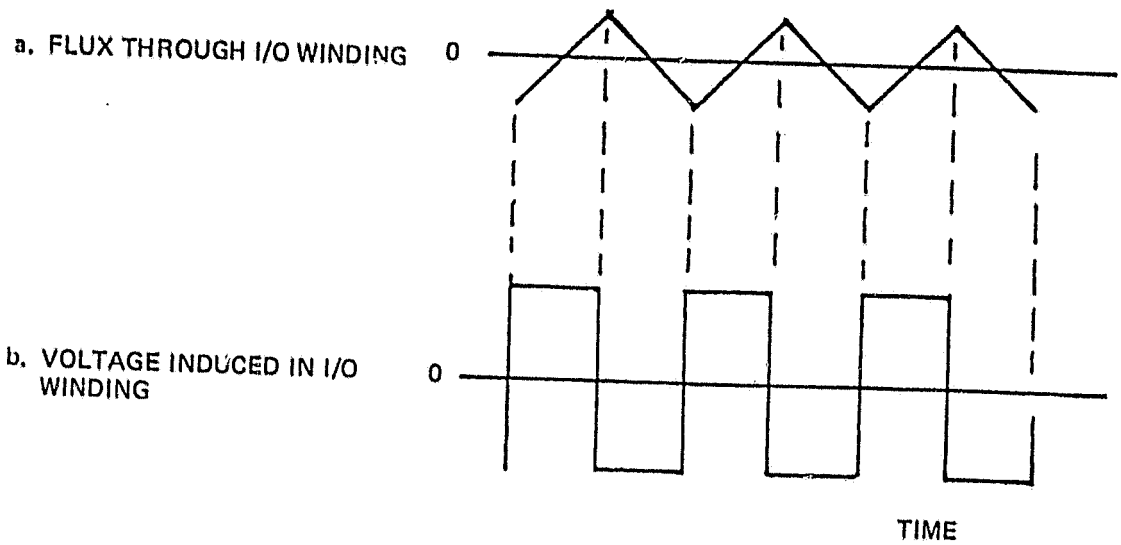

Figure 3.2. Flux and Voltage Waveforms

A simple model of the output circuit includes a voltage source, the system load, and the input/output winding inductance. Because the large fluxes necessary for high power density and efficiency require a small air gap, the i/o winding inductance is large. The i/o winding resistance is therefore assumed to be small compared to the impedance of the i/o winding inductance and is neglected in this model.

A schematic of this single rotor system during generator operation is shown in Figure 3.3. The field current I_{FA} produces magnetic flux which is coupled through the rotor to the i/o windings. As the rotor turns, the changing magnetic flux in the i/o coils induces a voltage V_A in the i/o coils. V_A drives a circuit consisting of the winding (motor) inductance L and the load R_L, which is assumed resistive.

When the inductor alternator is used as a motor (Figure 3.4), an electrical power supply supplies a time varying current to the i/o winding. The flux produced by this current combines with the flux produced by the field current; this total time varying flux is a rotating flux wave in the air gap between the rotor and the stator. Since the rotor is made of ferro-magnetic material, the rotor teeth are forced to rotate with the flux wave. This force produces a torque about the motor shaft, turning the flywheel.

3.2 DUAL ROTOR

The unique aspect of the CSDL dual field concept is the use of dual rotors to eliminate the undesirable effect of the i/o winding inductance. This undesirable effect is a voltage component V_L, produced by the current I_1 flowing through the i/o winding, which is out-of-phase with the current I_1. This reactive component of power wastes machine capacity and complicates the commutation process. Subtracting a voltage V_B, at the same frequency and phase as V_L, from

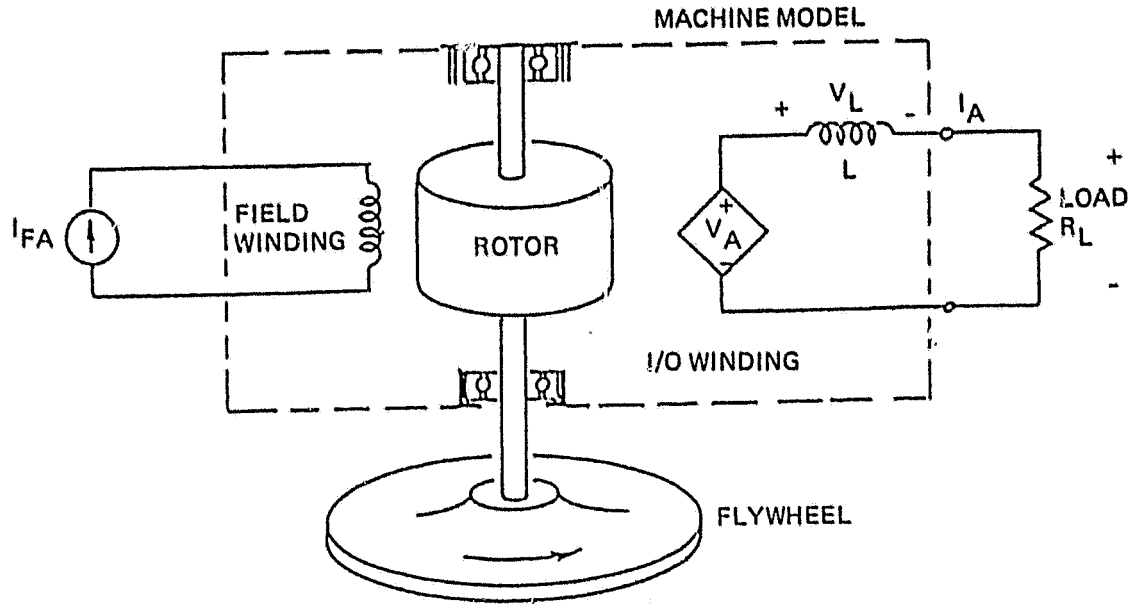

Figure 3.3. Generator Operation

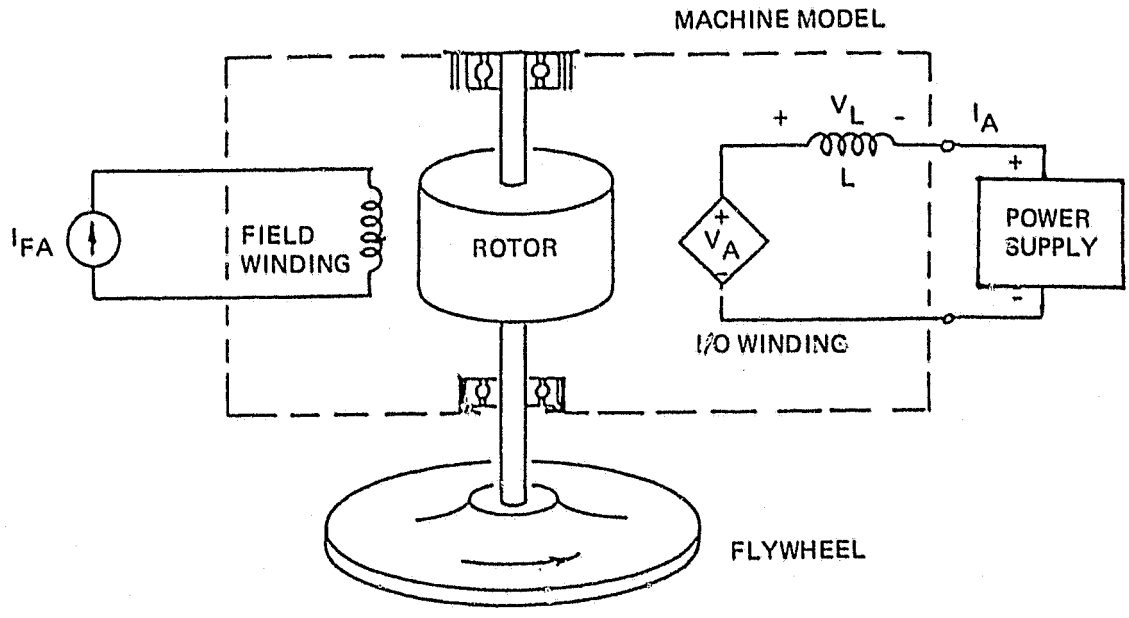

Figure 3.4. Motor Operation

the output voltage will cancel V_L, eliminating the reactive component of power. The output voltage and current will then be in phase, simplifying commutation.

The CSDL concept uses a second rotor and stator (Rotor-B), as indicated in Figure 3.5, to generate the voltage V_B. If the second rotor is on the same shaft as the first, but the stator windings are angularly displaced so that V_B leads V_A by 90°, the generated voltage V_B will always have the proper phase relationship to cancel V_L. The proper amplitude for V_B can be obtained by adjusting the field current I_{FB} in the second stator. When I_{FA} and I_{FB} are adjusted correctly, the waveforms shown in Figure 3.6(a-f) are generated.

The contribution to the output current of one phase (I_1) of the inductor alternator can now be calculated. There are two impedances in the model, ωL of the motor inductance and Z_L of the load. The fundamental frequency (ω) of $V_A + V_B$ is equal to the shaft speed multiplied by the number of rotor teeth. Because the shaft speed is high, $\omega L >> Z_L$. Neglecting Z_L compared to L gives the current as:

$$I_1(t) = \frac{1}{L}\int V_L(\tau)d\tau,$$

where V_L is the voltage across the inductor. However, since V_B is set so that $V_B = V_L$,

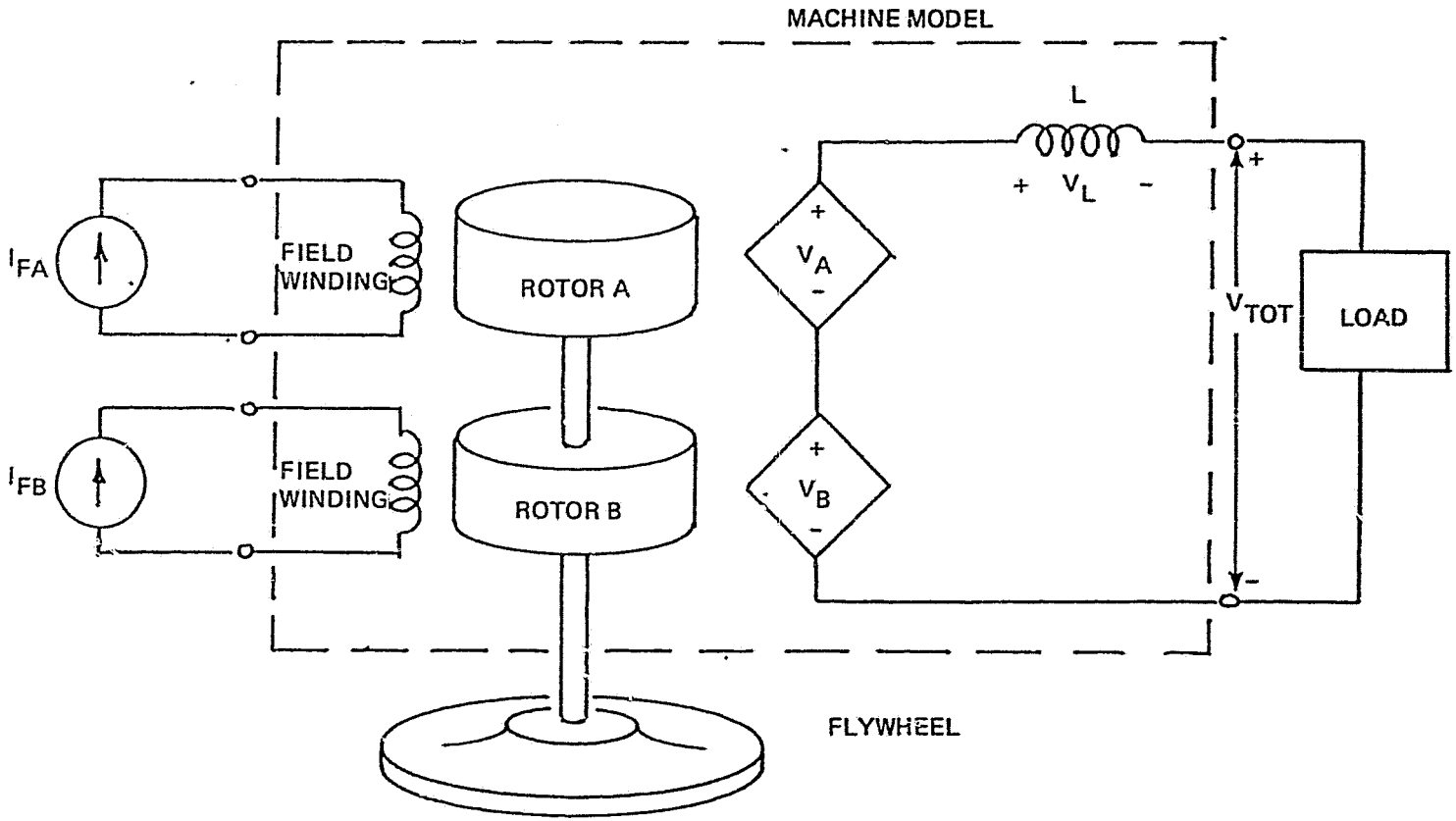

Figure 3.5. Dual Rotor Inductor Alternator

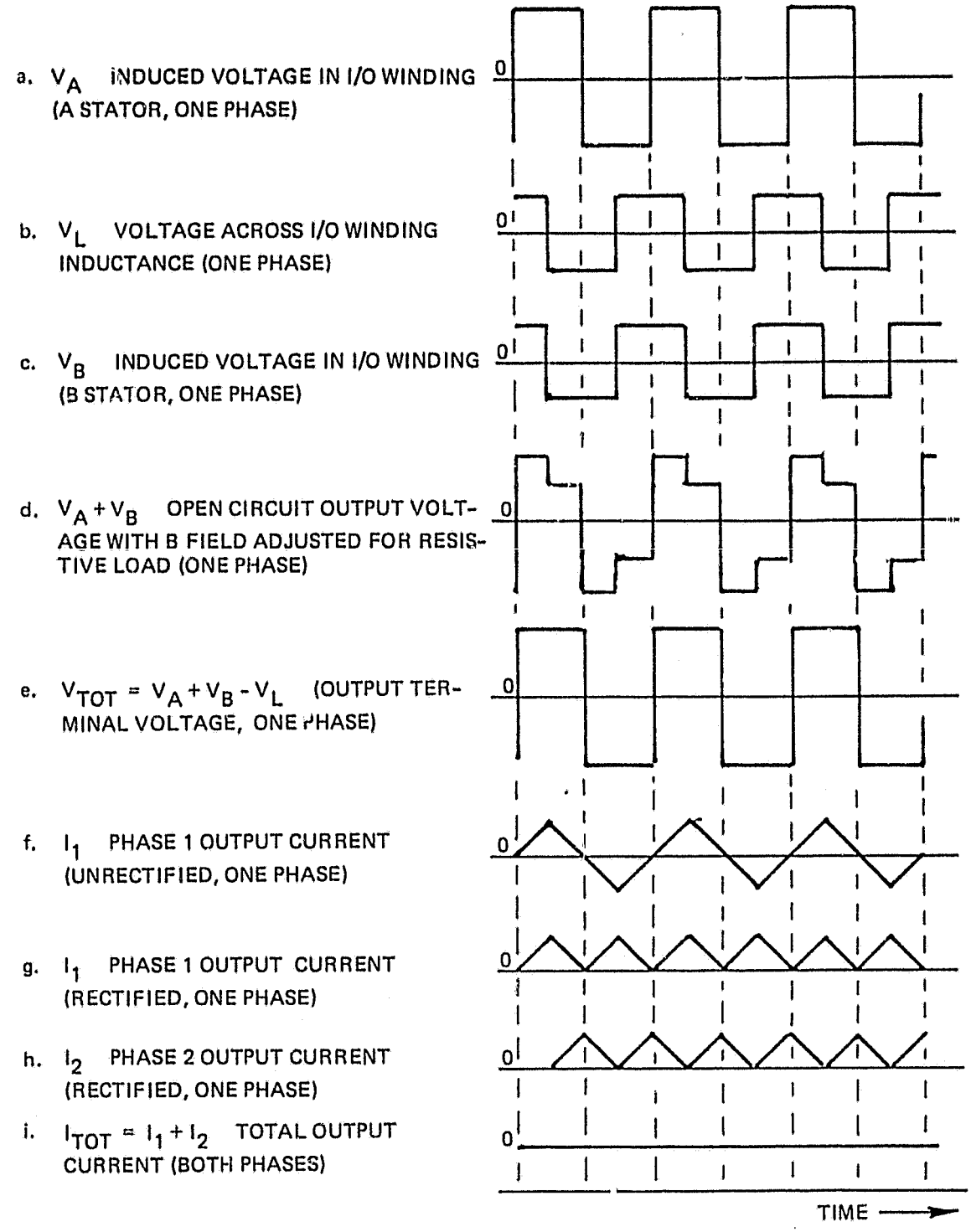

Figure 3.6. Inductor Alternator Waveforms

the current is equivalently given by:

$$I_1(t) = \frac{1}{L}\int V_B(\tau)d\tau.$$

For the square wave V_B, this gives the triangular wave I_1 as shown in Figure 3.6(f), which is the contribution of one phase to the total output current.

3.3 DUAL PHASE

Two output phases are used to produce DC output. The output current from the single phase inductor alternator has the form shown in Figure 3.6(f). With rectification this becomes the waveform shown in Figure 3.6(g). Since DC output is desired, a similar current waveform shifted by 90° is needed. This can be generated by a second set of i/o windings on each stator. The second set is wound so that the outputs of the two sets are identical but out of phase with each other by 90°. The current from both phases, when added together, is then DC. These waveforms are shown in Figure 3.6(g-i). A schematic of the dual phase, dual rotor inductor alternator is shown in Figure 3.7.

3.4 FIELD MODULATION

The inductor alternator can convert variable speed mechanical energy to and from variable frequency electrical energy by the use of field modulation. Field modulation is obtained by driving the field windings with alternating current at the desired modulation frequency. The generated voltage waveform produced without modulation acts as a carrier for the modulated waveform.

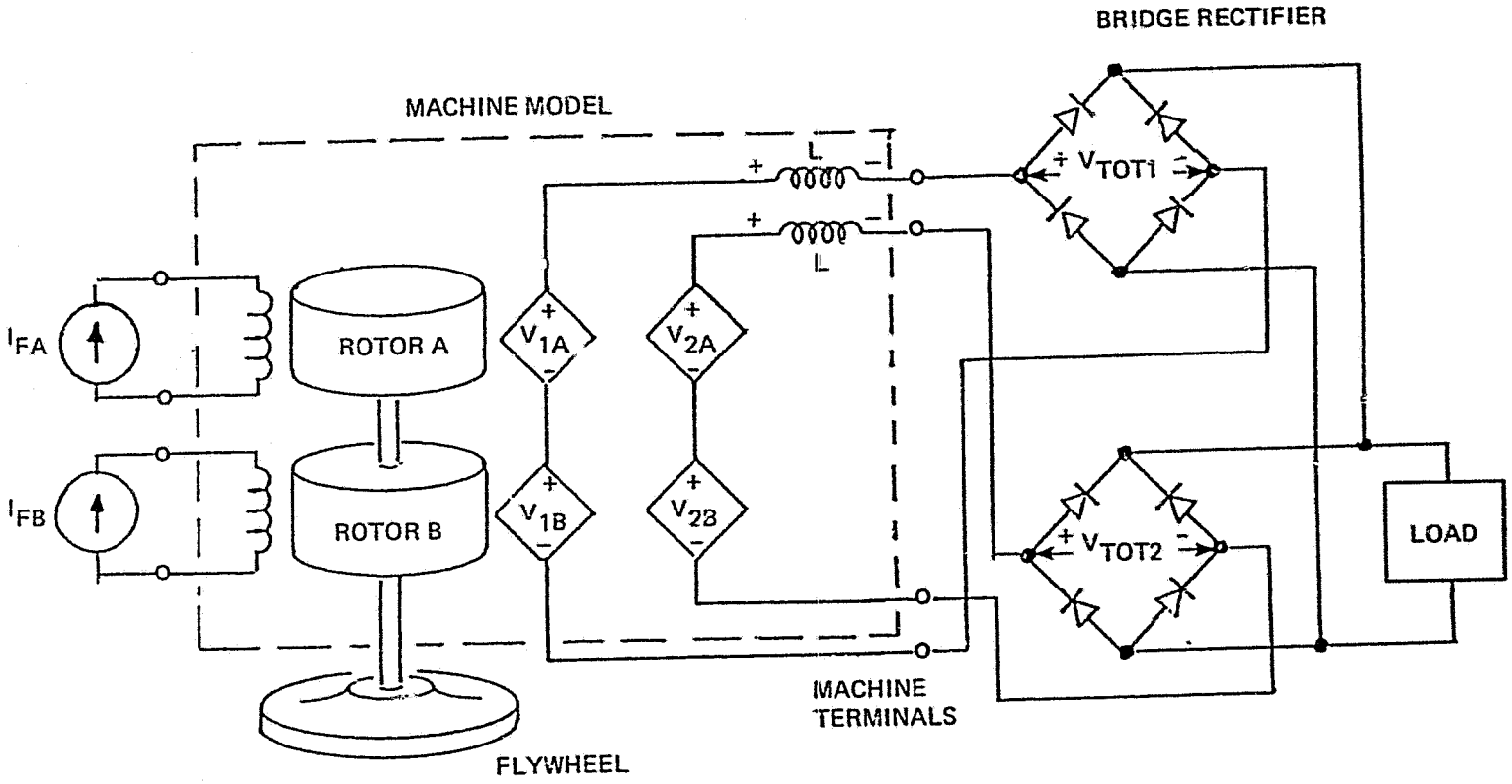

Figure 3.7. Dual Phase, Dual Rotor Inductor Alternator

There are now two frequencies of interest in the system. The first is the modulation frequency ω_m, the frequency at which the converter will interface with the electrical grid. The second is the alternator frequency ω_a. As noted before, this frequency is determined by the shaft speed and number of rotor teeth.

The system is designed with $\omega_a >> \omega_m$. The alternator frequency ω_a then acts as a high frequency carrier for the modulation frequency ω_m. The larger the ratio of ω_a to ω_m, the better the demodulated output current and voltage waveforms will have the frequency content (energy spectral density) of the modulating waveform. Field modulated waveforms for generator operation are shown in Figure 3.8. A more extensive discussion of field modulation and inductor alternators is contained in Reference 2.

3.5 CONTROLLER

The controller has three functions. First, it must protect the inductor alternator from excessively high voltages or currents (over-voltage and over-current protection). Second, in applications where the inductor alternator is coupled to a utility line, the controller must synchronize the inductor alternator with the line and control the amplitude and phase of the load current. Third, to achieve maximun efficiency and minimum electromagnetic interference (EMI) generation, the controller must keep the generated voltage in phase with the current.

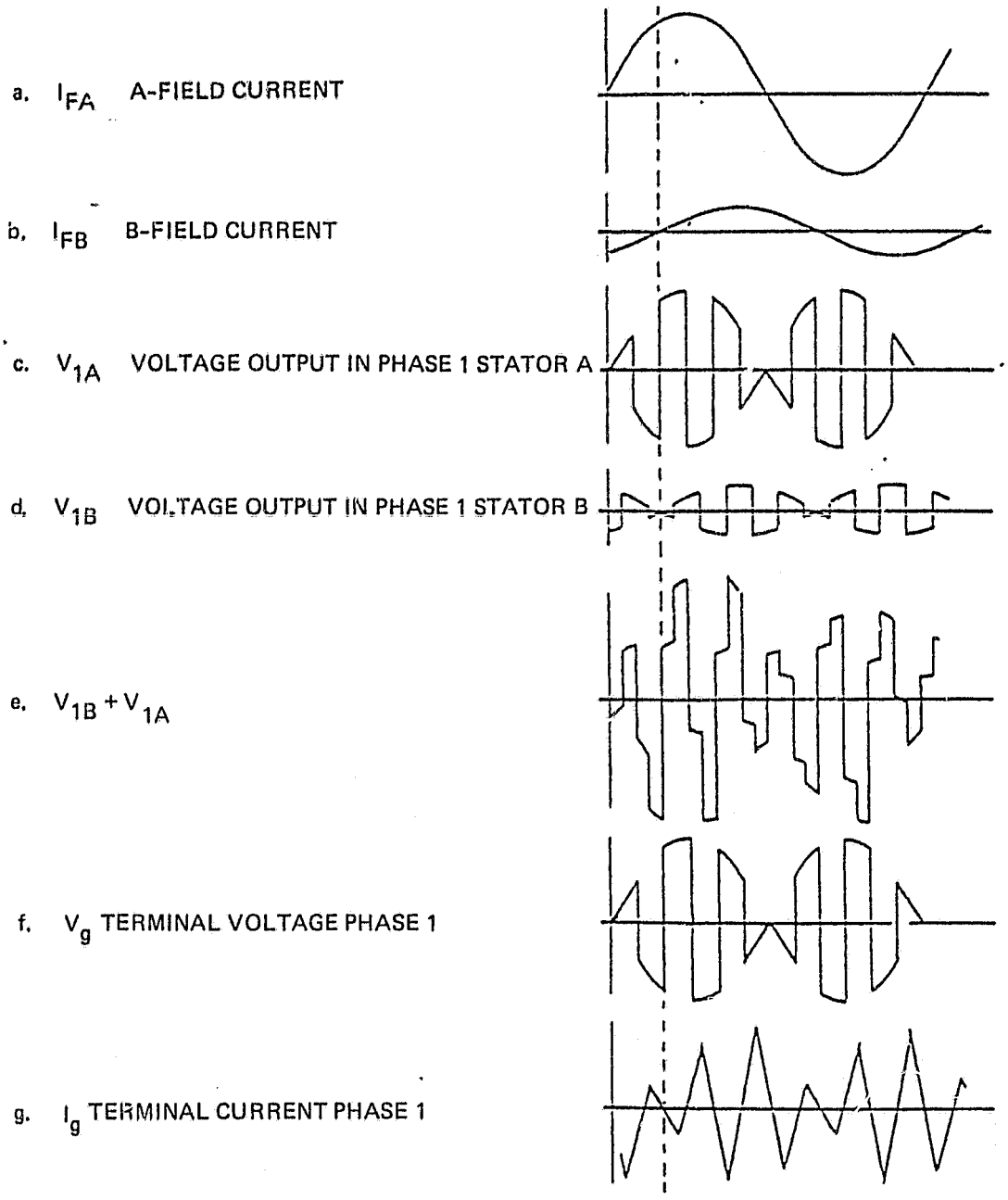

Figure 3.8. Field Modulated Waveforms
(Single Phase)

A block diagram of the controller is shown in Figure 3.9. The controller monitors 1) the line voltage V_o and current I_o, 2) the generated current I_g of each phase of the inductor alternator, 3) the inductor alternator stator position, and 4) a signal indicating desired line current I_R or voltage V_R. The controller uses this information to 1) set the two field currents I_{FA} and I_{FB}, 2) demodulate the inductor alternator output if necessary, and 3) rectify the inductor alternator generated current.

The block diagram shows the three main subsystems of the controller, 1) the switching and firing circuits, 2) the A-field feedback control, and 3) the B-field feedback control. V_g and I_g are inputs from the inductor alternator to the switching circuit (demodulator) whose output is a lower frequency or DC voltage and current (V_o, I_o). The switching circuit is switched by a firing circuit which has as inputs the line current I_o and voltage V_o, and the rotor position.

The B-field feedback control circuit uses an encoder which measures the relative positions of the rotor and stator to determine the zero-crossings of the inductor alternator generated voltage V_g. Output current zero-crossings are determined by a polarity indicator on sensed current. Any phase difference between the current and voltage produces an error signal. This error signal is then fed to the B-field, driving the machine to correct the error.

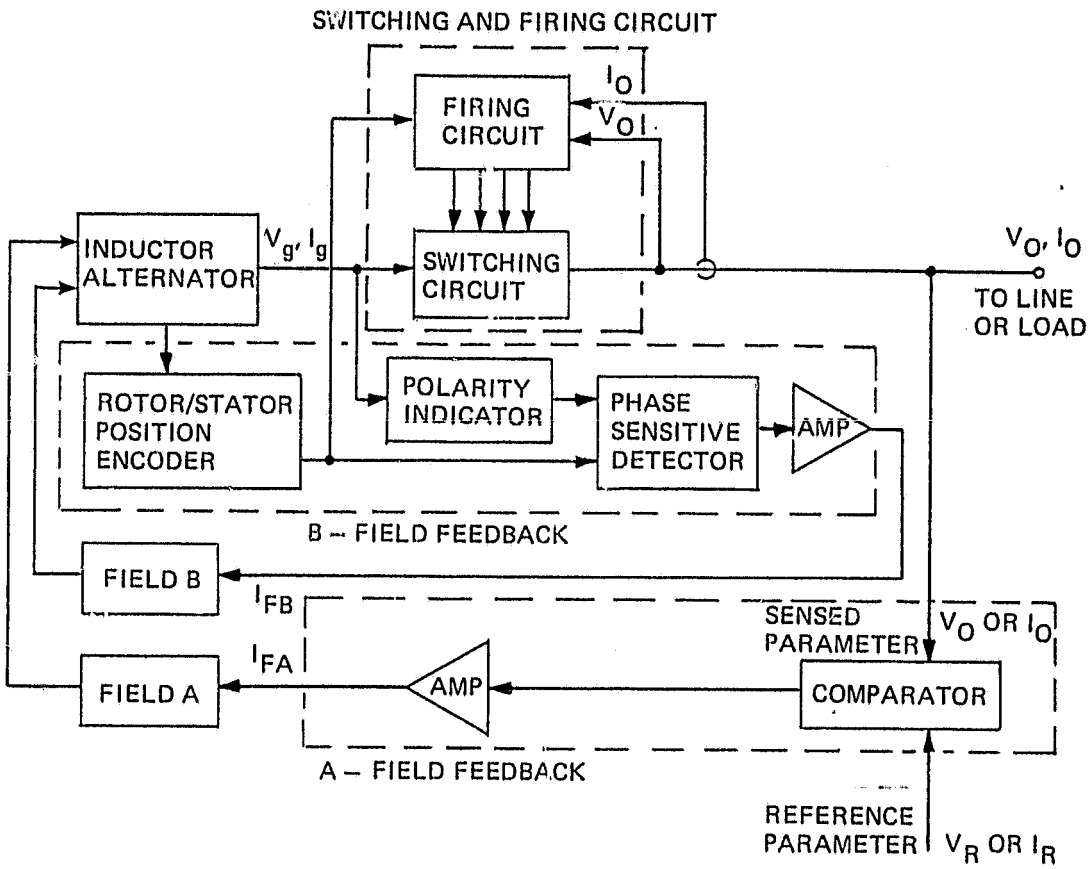

Figure 3.9. Controller Block Diagram

The A-field feedback control circuit modulates the higher-frequency (ω_a) generated voltage V_g at the frequency ω_m of the lower frequency voltage V_o and controls the amplitude of the generated voltage V_g. The control circuit measures the amplitude difference between a reference or desired level (V_R or I_R) and the sensed line parameter (V_o or I_o). The resulting difference signal drives the A-field to adjust the sensed parameter toward the reference level. If the switching circuit is coupled to a line, line current I_o is sensed and compared to a reference level for the current I_R. In a stand-alone mode, voltage V_o would be sensed and compared to a reference voltage V_R.

4. CSDL INDUCTOR ALTERNATOR DESIGN

4.1 MECHANICAL DESIGN

The mechanical design of the inductor alternator is conventional; it has a horizontal shaft and an open frame (Figure 4.1). There are two mechanically identical stators and two identical rotors mounted along a common shaft. The stators and rotors are both aligned mechanically (Figure 4.2). The shaft is supported at both ends by ball bearings mounted in the stator housing.

The stators and rotors are constructed from stamped 0.036 cm. Allegheny-Ludlum laminations that are stacked and bonded together. The stators are stamped with 24 winding slots, are 4.1 cm. thick, have an outside diameter of 20.8 cm., and have a 10.12 cm. inside diameter. Each rotor has six teeth as shown in Figure 4.2 [2]. The rotors have the same thickness as the stators, 4.1 cm., and have a radius of 9.94 cm. The radial air gap is 0.09 cm., equal to the difference between the rotor radius and the stator inside radius.

Allegheny-Ludlum 4750 high-nickel steel was chosen for the lamination material because of its high strength and high permeability. High strength laminations are necessary due to high rotor speeds. High permeability simplifies the analysis of the magnetic circuit (section 4.3) and increases power density and efficiency.

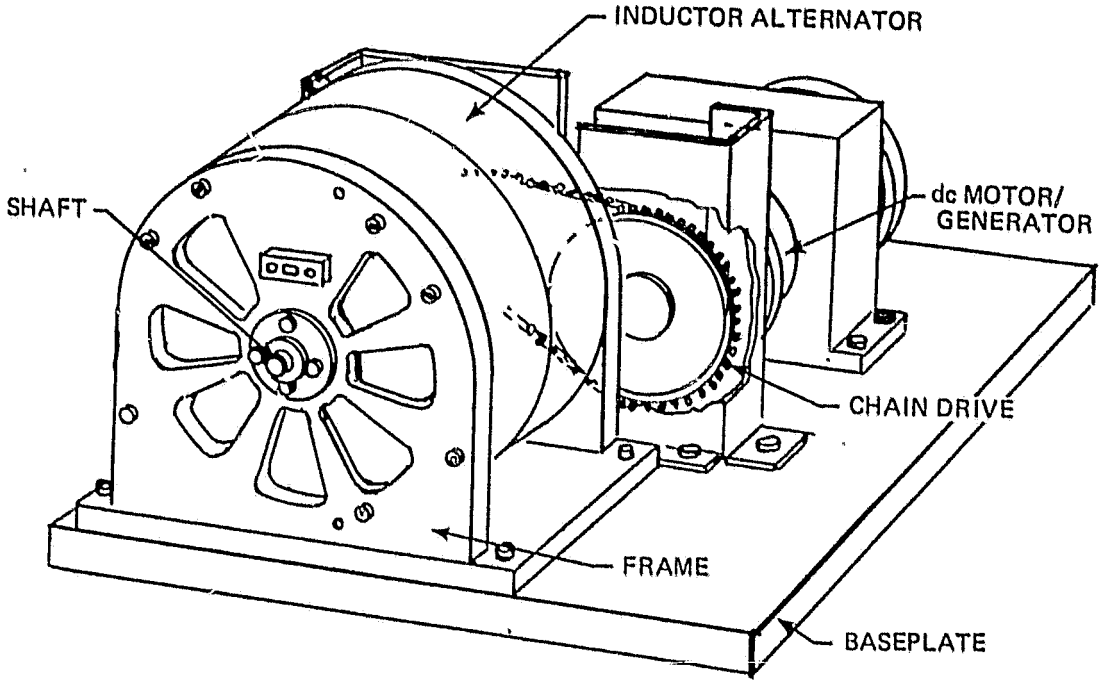

Figure 4.1. CSDL Inductor Alternator

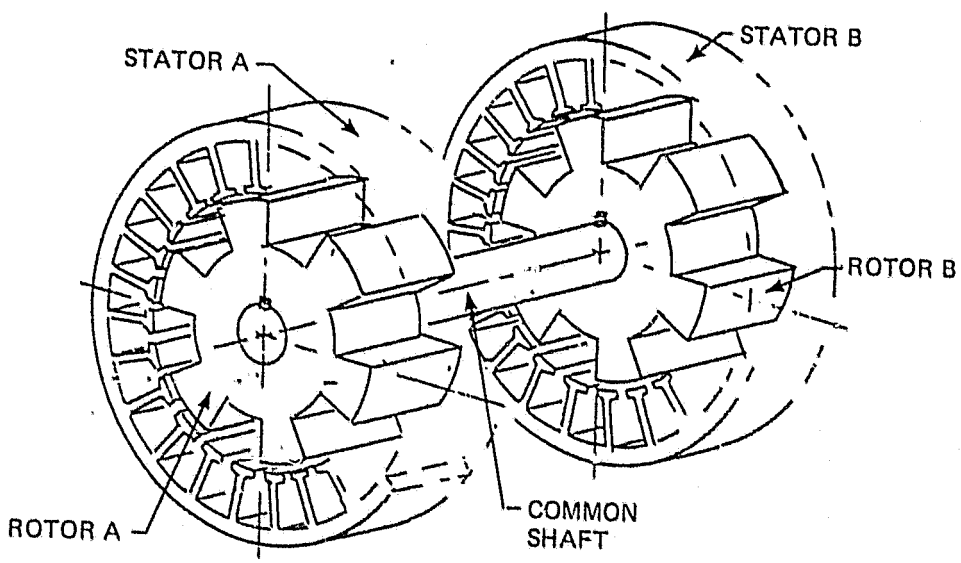

Figure 4.2. Cutaway View of Stator and Rotor Alignment

The major design challenge was the requirement for tight tolerances on the radial air gap between rotor and stator. Since the nominal flux density in the stator teeth is near the magnetic saturation level of the alloy, small variations in the air gap length produce magnetic saturation. Therefore, the air gap was held to ±0.005 cm. of the nominal 0.09 cm. gap.

In order to design a 0.005 cm. total air gap tolerance, a tolerance analysis was performed. Bearing, rotor, stator, housing, and alignment tolerances all affect the air gap tolerance. From this analysis, the decision was made to do the final machining of the rotors after they had been keyed and bonded to the shaft. The final rotor diameter is within 0.00025 cm. of nominal with a concentricity between the shaft and rotor of 0.0005 cm. total indicated reading (TIR).

After machining, the shaft assembly was balanced by E.E. Lindskog Co. of Bedford, MA. The original unbalance was 7.5 gram-cm (worst side). The residual unbalance is 1.2 gram-cm (worst side), which is within the quality grade established for tape recorders or small armatures.

Both the inside diameters and the outside diameters of the stators have tolerances of ±0.00025 cm. The inside diameters are concentric to the outside diameters within 0.0005 cm. TIR.

The stator housing is split into two sections to allow for adjustments of stator position. However,

this adjustment capability was not used during the actual assembly and test. The housing sections were fabricated separately, then pinned together for the final machining of the inside diameter. The housing inside diameter has a tolerance of ±0.00025 cm., and the nominal diameter is 0.001 cm. greater than the nominal diameter of the stator.

The housing end plates were also fabricated separately then pinned to their corresponding housing sections before final machining of the bearing location holes. The diameters of the bearing holes have a 0.00025 cm. tolerance. The concentricity between the housing inside diameter and the bearing holes is 0.0005 cm. TIR. The bearings are standard DFSS-16 bearings with an eccentricity of 0.0013 cm.

A complete set of manufacturing drawings has been provided to NASA/LeRC.

4.2 WINDINGS DESIGN

Each stator carries three sets of windings: field, input/output-1, and input/output-2. The winding pattern is shown in Figure 4.3 for 8 stator teeth. The pattern is repeated for the remaining 16 teeth.

Figure 4.3 indicates the reference direction of current in the windings. The stators are wound so that a positive current flow is in the direction shown by the arrows. The windings on stator-B are connected to the windings on stator-A so that the voltage V_B

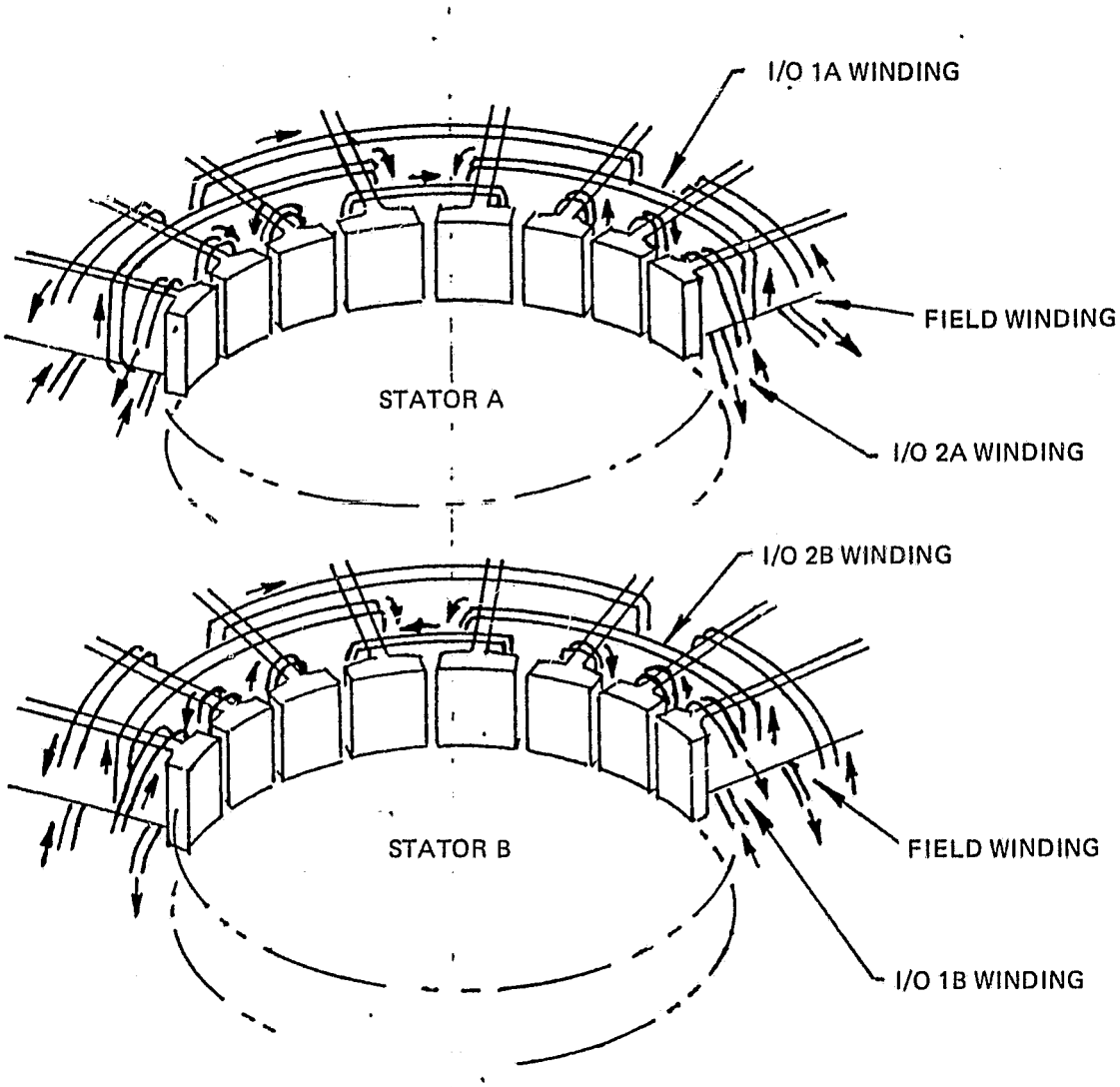

Figure 4.3. Winding Pattern

produced from stator-B has the correct phase relationship to cancel the voltage V_L from the i/o winding inductance (Section 3.2).

All winding wire is copper magnet wire; the wire gauge and number of turns per coil for the six windings are given in Table 4.1. Note that the input/output winding wire is composed of three individual wires wound together.

4.3 MAGNETIC DESIGN

The magnetic circuit of the inductor alternator is comprised of the stator, rotor, air gap, and windings. The magnetic circuit can be adequately modeled as a time varying, lumped parameter system.

Table 4.1 Inductor Alternator Winding Data

WINDING	TURNS/COIL	AWG[1]	NO. COILS
FIELD-A	200	#22	6
FIELD-B	200	#22	6
INPUT/OUTPUT-1A	25	3x(#23)	6
INPUT/OUTPUT-1B	25	3x(#20)	18
INPUT/OUTPUT-2A	25	3x(#20)	18
INPUT/OUTPUT-2B	25	3x(#23)	6

[1]American Wire Gauge

The lumped parameter circuit model for the section of stator-A shown in Figure 4.3 is given in Figure 4.4. There are magnetomotive forces (MMF) due to the field, input/output-1, and input/output-2 windings. The magnetic path consists of the gap reluctances R_g between the rotor and stator and the leakage reluctance R_ℓ between the stator teeth. The reluctance of the iron portions of the path are neglected.

The leakage reluctance R_ℓ is calculated from an infinite parallel plane approximation. Using this approximation,

$$R_\ell = \frac{d}{\mu_0 A},$$

where d = gap between stator teeth
μ_0 = permeability of air
A = area of gap between stator teeth.

The gap reluctance at a stator tooth R_g is a function of the rotor position. The minimum value of R_g is calculated as above and is

$$R_g = \frac{g}{\mu_0 A},$$

where g = gap distance
A = stator tooth area.

The maximum reluctance is approximately ten times this value. Since one rotor tooth covers two stator teeth, R varies in a trapezoidal manner between the

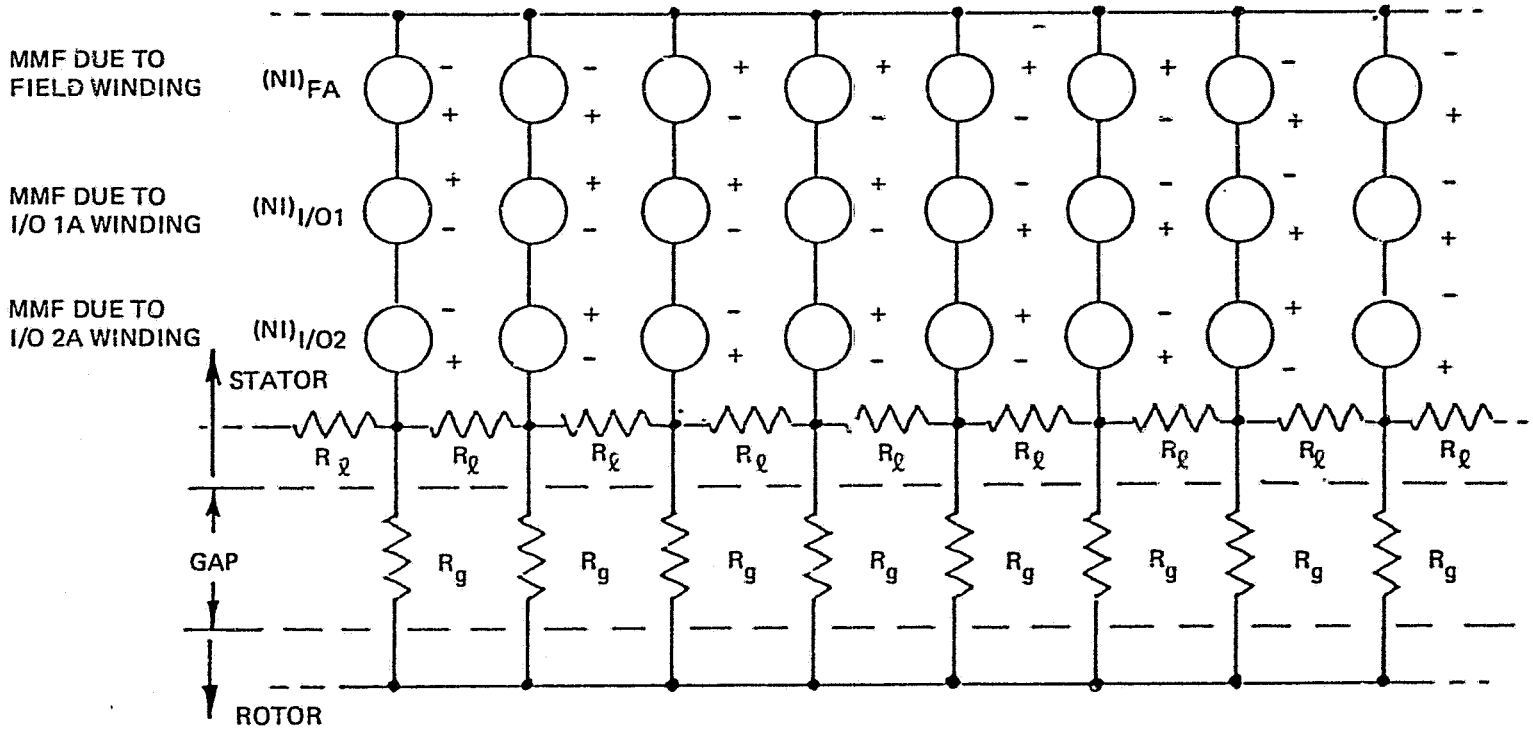

Figure 4.4. Lumped Parameter Magnetic Circuit

maximum and minimum values as the rotor turns. This trapezoidal waveform for the reluctance R_g across the gap at a stator tooth is shown in Figure 4.5.

The magnetic circuit can be solved for the time varying flux in each path. From the solution for the flux, the output voltage can be calculated and, given the load, the output current can be calculated. The effect of various design parameters (shaft speed, geometry, windings) on system performance (output voltage and current) can also be determined.

One important characteristic is the open circuit output voltage. When the ouput circuit is opened, no currents flow in the in the i/o windings; the magnetic circuit analysis is simplified. A plot of the predicted output voltage versus field current, neglecting saturation, is shown in Figure 4.6.

Another important characteristic is the onset of magnetic saturation in the stator teeth. Saturation in the Allegheny-Ludlum alloy occurs at a magnetic field density of about 1.5 tesla. Field currents of about 1 amp will produce this field density. When the stator teeth become saturated, the reluctance of the teeth is no longer negligible, invalidating the model. Therefore, large deviations between model predictions and experimental results are expected at current levels greater than 1 amp (Section 5.3).

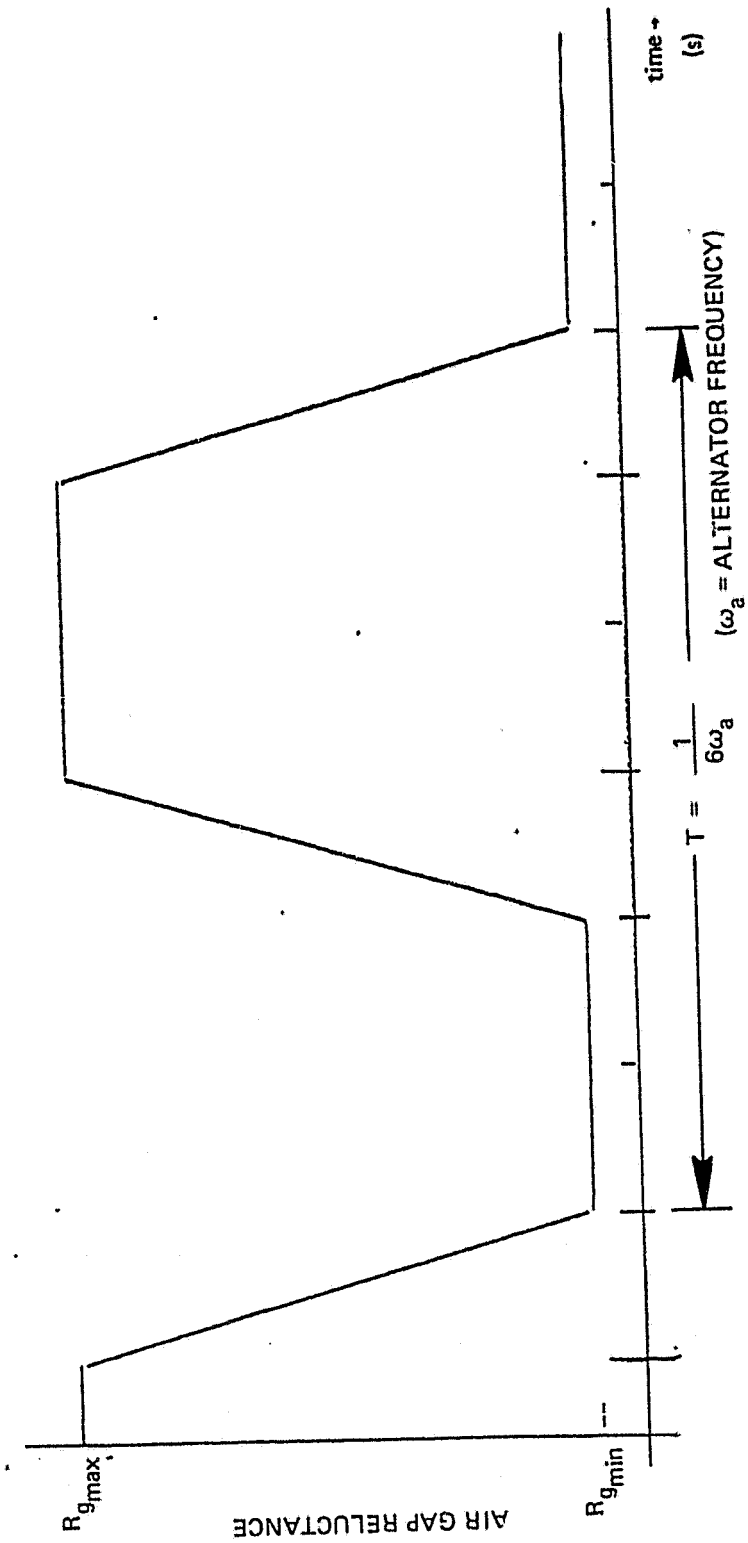

Figure 4.5. Gap Reluctance versus Time

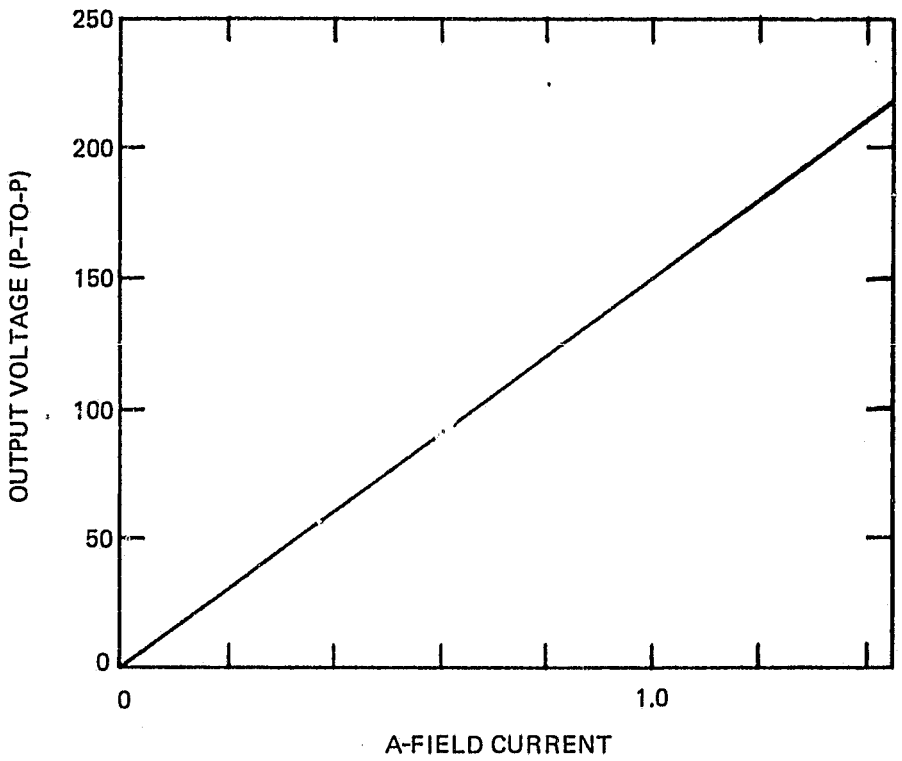

Figure 4.6. Peak-to-Peak Open Circuit Voltage versus I_{FA} (A-Field Current)

4.4 CONTROLLER DESIGN

Although the design and implementation of the controller is not included in the NASA/LeRC contract, a description of its partial implementation is included here. The controller can be divided into three subsystems: 1) the firing and switching circuits, 2) the A-field feedback control, and 3) the B-field feedback control.

The feedback control loops for the A and B-fields were not closed electronically as indicated in Figure 3.9. The field currents were controlled manually during the test. The A-field current I_{FA} was set to produce the desired voltage output and the B-field was adjusted to minimize the true rms ripple. This corresponds to setting V_B equal to V_L as discussed in Section 3.2. This process is described in the discussion of the test procedures (Section 5.1)

The switching and firing circuits of Figure 3.9 were built. A schematic, showing the important features of the circuits, is contained in Figure 4.7.

The switching circuit is controlled by the firing circuit. The switching sequence depends on the mode of operation of the inductor alternator, motor or generator; the zero-crossings of the output voltage V_o; and the zero-crossings of the generated voltage V_g. The firing circuit uses a one-of-eight decoder to process the input information and drive the switching circuit. The decoder has three inputs: one from an exclusive OR

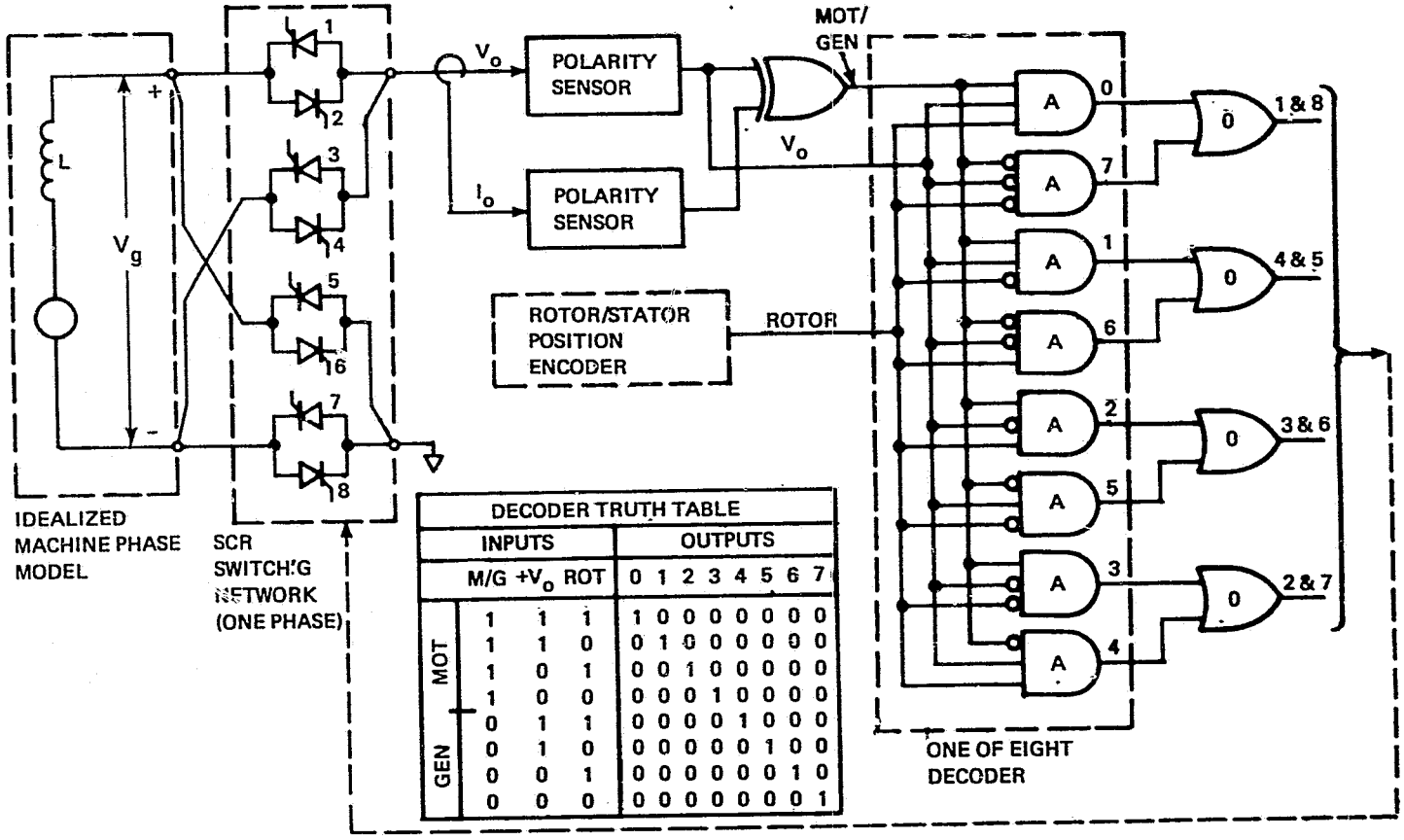

DECODER TRUTH TABLE

INPUTS				OUTPUTS							
	M/G	$+V_o$	ROT	0	1	2	3	4	5	6	7
MOT	1	1	1	1	0	0	0	0	0	0	0
	1	1	0	0	1	0	0	0	0	0	0
	1	0	1	0	0	1	0	0	0	0	0
	1	0	0	0	0	0	1	0	0	0	0
GEN	0	1	1	0	0	0	0	1	0	0	0
	0	1	0	0	0	0	0	0	1	0	0
	0	0	1	0	0	0	0	0	0	1	0
	0	0	0	0	0	0	0	0	0	0	1

Note: SCR Switching is Duplicated for Second Machine Phase

Figure 4.7. Switching and Firing Control Circuits with Decoder Truth Table

gate that indicates motor or generator operation, one from a polarity sensor that indicates the polarity of the output voltage V_o,and one from the rotor position sensor that indicates the polarity of the inductor alternator generated voltage V_g. The eight outputs of the decoder, labelled 0-7, are inputs to four OR gates which operate the silicon controlled rectifier (SCR) switches of the switching circuit.

The truth table for the decoder is shown at the bottom of Figure 4.7. A "1" in the motor/generator column (marked M/G) denotes motor operation; a "0" denotes generator operation. In the output voltage column (marked $+V_o$), "1" denotes positive output voltage and "0" negative output voltage. In the rotor column (marked ROT), "1" denotes that the rotor position indicates positive generated voltage V_g, and a "0" indicates negative generated voltage.

The decoder is implemented by a group of AND gates and inverters as shown in Figure 4.7. The output of the decoder is shown driving SCR switches, since the high-power applications expected require them. Transistor switches may be substituted in lower power applications.

5. CSDL INDUCTOR ALTERNATOR PERFORMANCE

5.1 TEST SET-UP

The inductor alternator was tested both as a motor and as a generator, using a DC motor to turn the inductor alternator in the generator test, and as a load in the motor test. As a generator, efficiency and output ripple were measured; as a motor, efficiency was determined. The original concept also envisioned the inductor alternator operating into a fixed frequency AC line (Section 2.2). Although the final design was not optimized for this use, during the test AC operation was demonstrated, and waveforms recorded.

For test purposes, the inductor alterntor is mounted on a common baseplate with a conventional DC motor, and coupled by a 5:3 speed increaser, using a belt drive (Figure 5.1). The DC motor is a 27-volt, 30-ampere, 7000 RPM aircraft motor manufactured by ESMCO.

5.2 GENERATOR PERFORMANCE

The measurement procedure for the generator test (see Figure 3.7) was conducted as follows:

1. The stationary resistance of the DC drive motor was measured across the motor terminals. The measured value was 0.196 ohms.

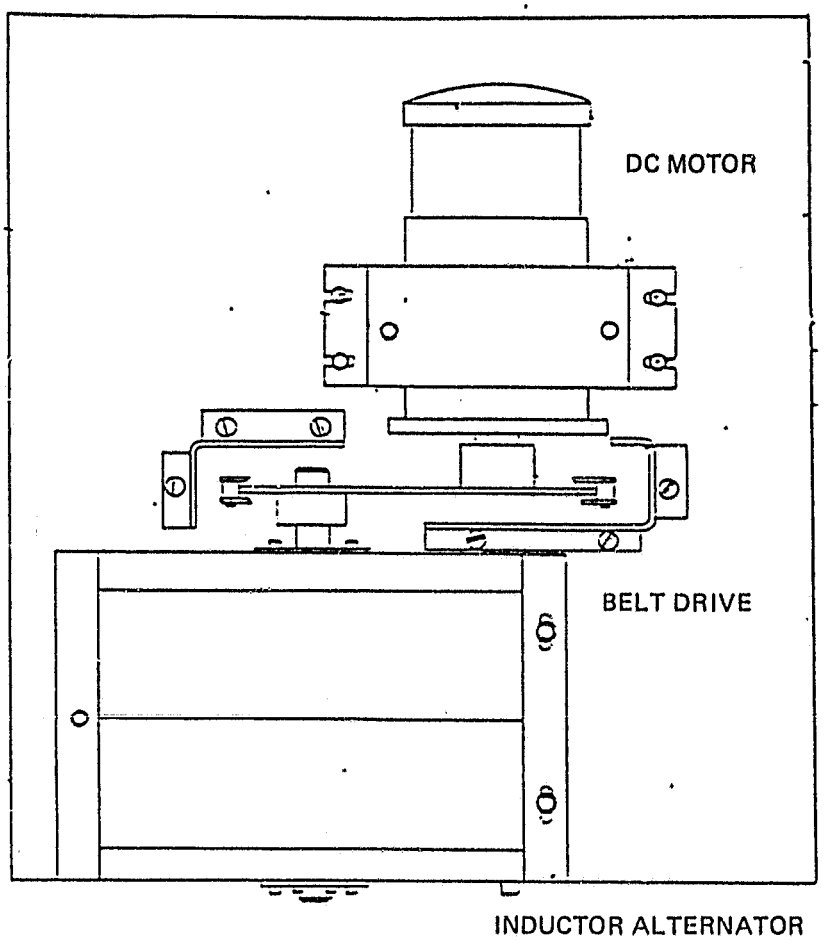

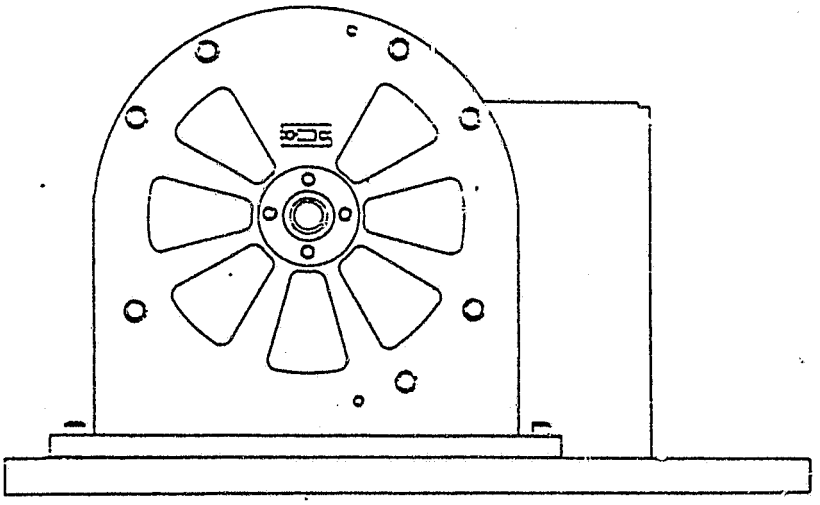

Figure 5.1. Inductor Alternator Test Bed

2. The inductor alternator was run with field excitation varied between 0 and 2.5 amps (fields connected in series), over the prescribed 5000-10000 RPM speed range. The input voltage and current of the DC motor were measured at 500 RPM intervals in this range.

3. Mechanical power, $P_m(\omega)$ is defined as the difference between input power ($V_{in} \cdot I_{in}$) as measured in (2) and the I^2R losses in the DC motor as determined by the current measured in (2) and the resistance measured in (1).

4. Input power as defined above was determined and plotted for various current levels in the field windings. Figure 5.2 indicates the result with both output winding circuits opened.

5. Tests under load were then performed into 12.5, 25, 30, and 100 ohm loads. Measurements were made with the A-field current set at 50, 100, 150, and 200% of the current level required for the onset of magnetic saturation in the stator (100% = 1.0 amp.). Measurements were made at 1000 RPM intervals between 5000 and 10000 RPM.

6. For each measurement, the B-field current was adjusted to minimize output ripple current as measured by a true rms digital multimeter (DMM). The output windings were connected in parallel as in Figure 3-7.

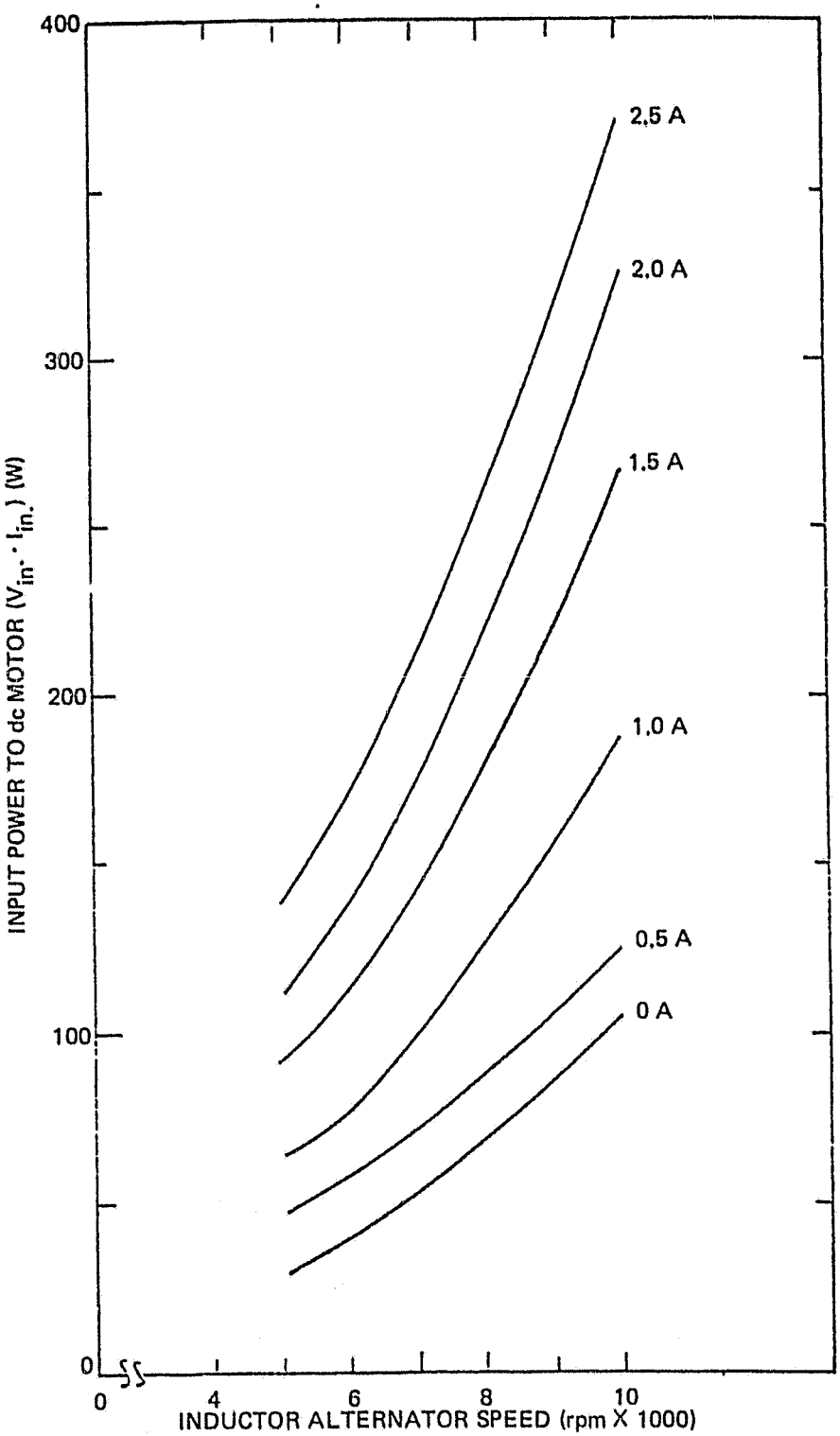

Figure 5.2. dc Motor Power versus Inductor Alternator Speed for Various Field Excitations with Input/Output Winding Circuits Open

7. In summary, the measurements made at each of the 1000 RPM intervals specified above were:
   a) Input voltage to the DC motor
   b) Input current to the DC motor
   c) Current in the A-field
   d) Current in the B-field
   e) Output (load) current
   f) Output (load) current ripple

In order to calculate net input power ($P_{net}(\omega)$), I^2R losses in the DC motor and mechanical losses measured in (3) were subtracted from the total input power to the DC motor ($V_{in} \cdot I_{in}$). The formula is thus $P_{net}(\omega) = V_{in} \cdot I_{in} - I^2_{in}R - P_m(\omega)$.

The output current waveform is shown in Figure 5.3 (a). The generated voltage has waveforms as in Figure 5.3 (b) [2]. These waveforms are closely comparable to the idealized design waveforms Figure 3.6.

The results were evaluated on the basis of three criteria: ripple, efficiency and power output. Figure 5.4 illustrates the ripple performance of the inductor alternator for two different loads and several levels of field excitation.

The important aspects of this graph are all explainable in terms of flux saturation in the inductor alternator iron. The overall upward trend in ripple as a function of increasing A-field excitation is directly attributable to saturation. It should be noted, for instance, that the curves for the 100 ohm load at 0.5

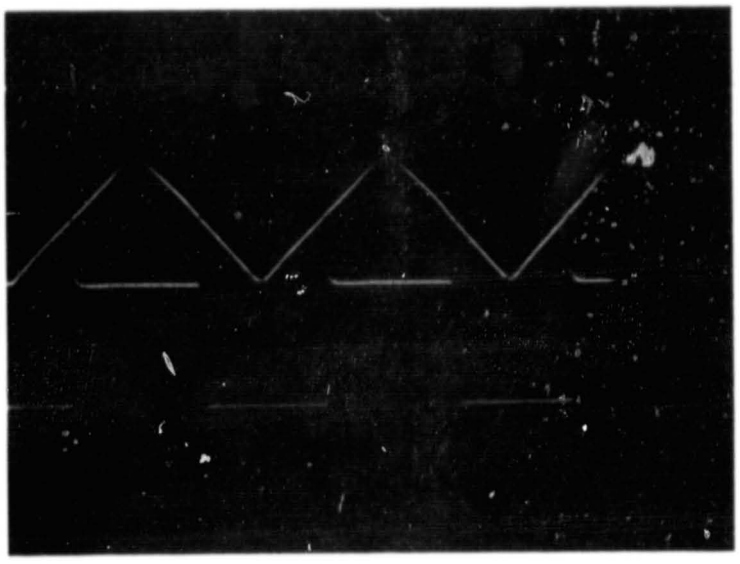

a. I_1 OUTPUT CURRENT FROM ONE PHASE (TOP)

V_{TOT} OUTPUT VOLTAGE FROM ONE PHASE (BOTTOM).
COMPARE WITH 3.6 (f), (e)

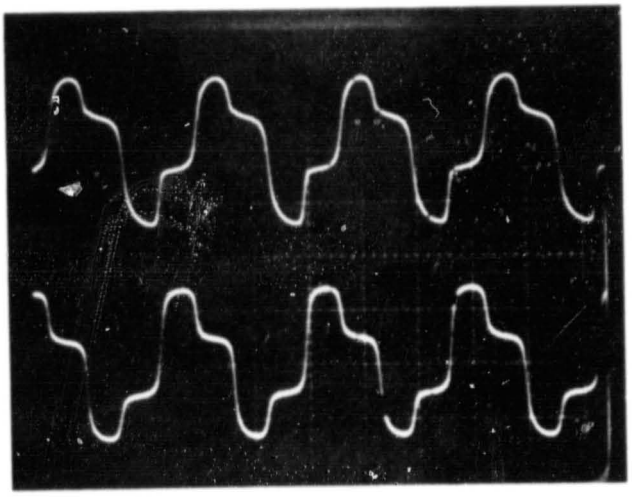

b. PHASE 1 $V_A + V_B$ (TOP)

PHASE 2 $V_A + V_B$ (BOTTOM)

Figure 5.3. Generator Test. Inductor Alternator Waveforms

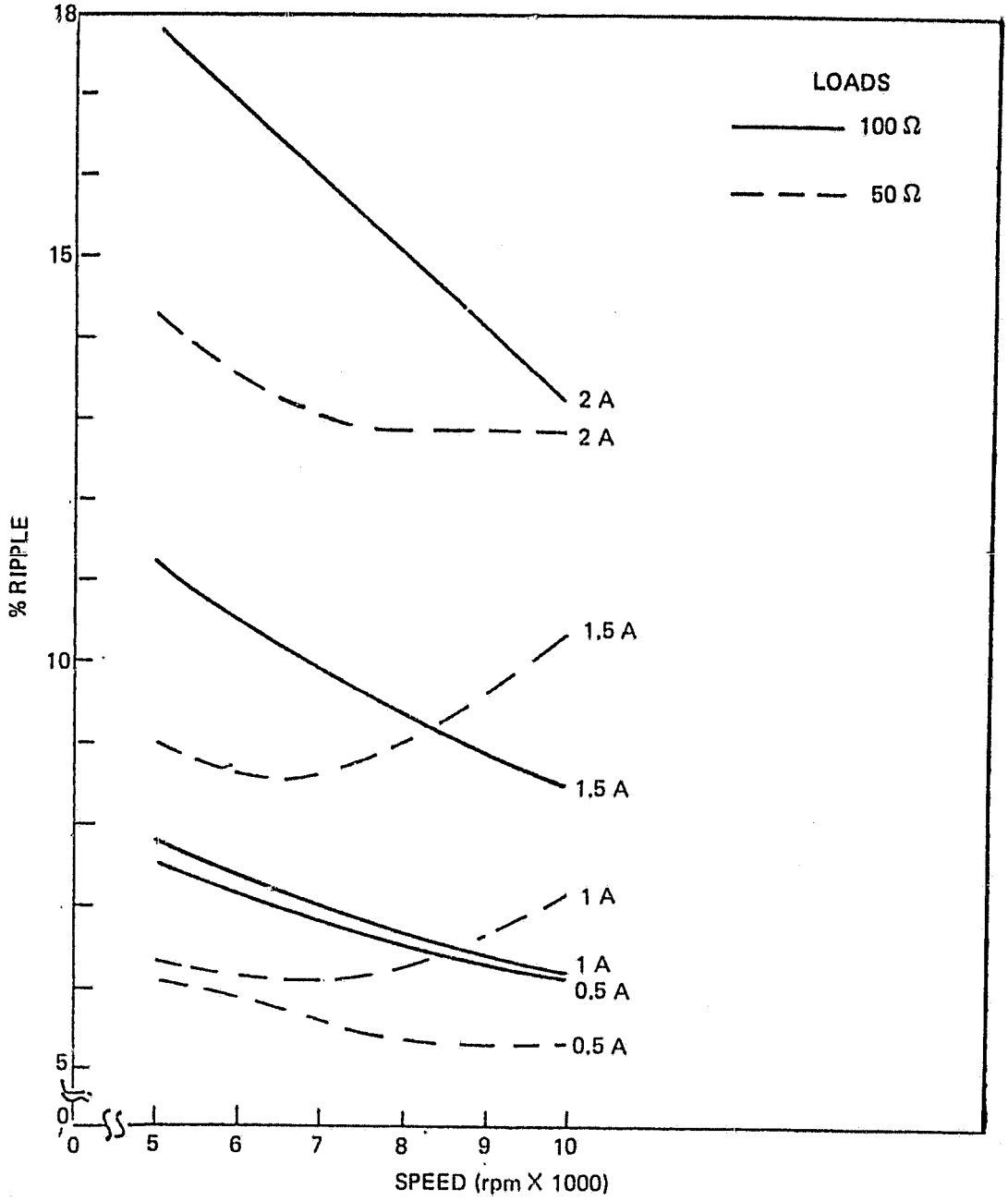

Figure 5.4. Generator Test. Output Ripple versus Inductor Alternator Speed for Various A-Field Current (I_{FA}) Levels and Loads

and 1.0 amp. excitation are virtually identical. As the excitation is increased above the level of saturation (1.0 amp.), ripple increases rapidly, as shown by the curves for 1.5 and 2.0 amps. At a given current level, the 100 ohm-load curves all trend downward as inductor alternator speed increases. This effect is caused by the output winding inductive reactance, which increases with generated frequency.

The curves for the 50-ohm load exhibit an additional phenomenon. The curve for nominal (1.0 amp.) excitation has a local minimum. The upward trend is due to saturation of the B-field stator. This effect is readily explained by the characteristics of the inductor alternator. Output voltage is proportional to rotor frequency, while output current is constant. Thus as speed increases, B-field field excitation must increase in order to maintain minimum ripple across the fixed load. The 50 ohm load requires twice as much current to maintain a given voltage, and as speed increases, the B-field stator begins to flux-saturate, increasing ripple.

The relation between ripple and output power is shown in Figures 5.5 and 5.6. As can be seen in Figure 5.5, ripple is relatively independent of power output up to the point at which saturation occurs, after which ripple increases dramatically. Notice that higher speeds produce lower ripple. For the 50 ohm load, saturation is reached more rapidly, and the ripple rises steeply.

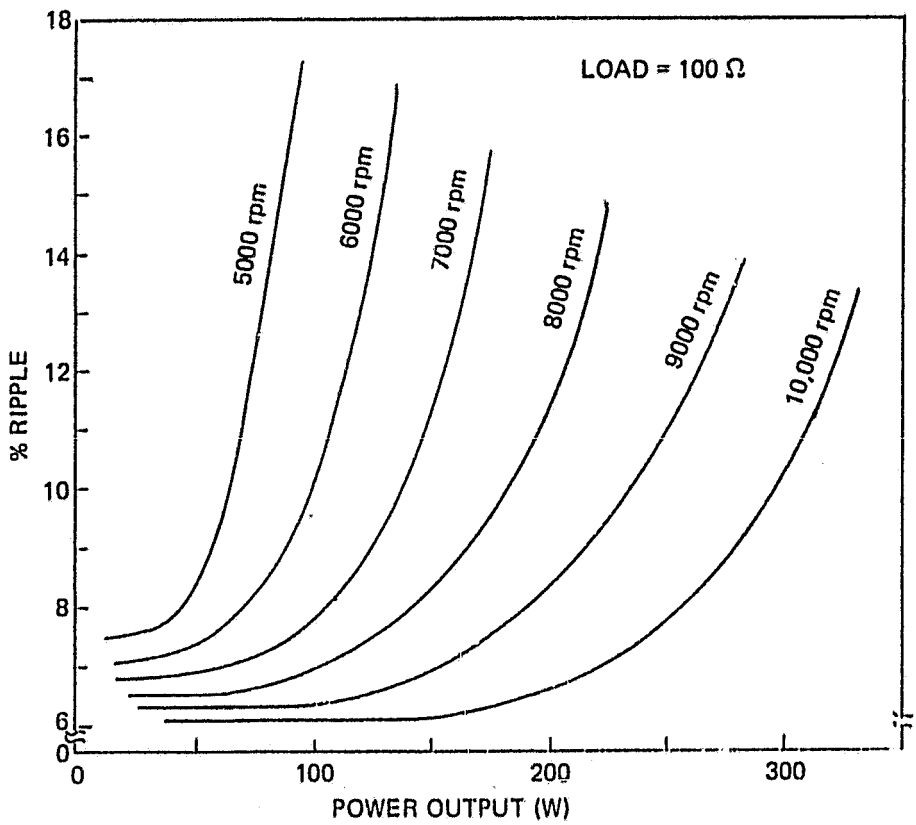

Figure 5.5. Generator Test. Output Ripple versus Output Power into a 100 Ohm Load with Speed as a Parameter

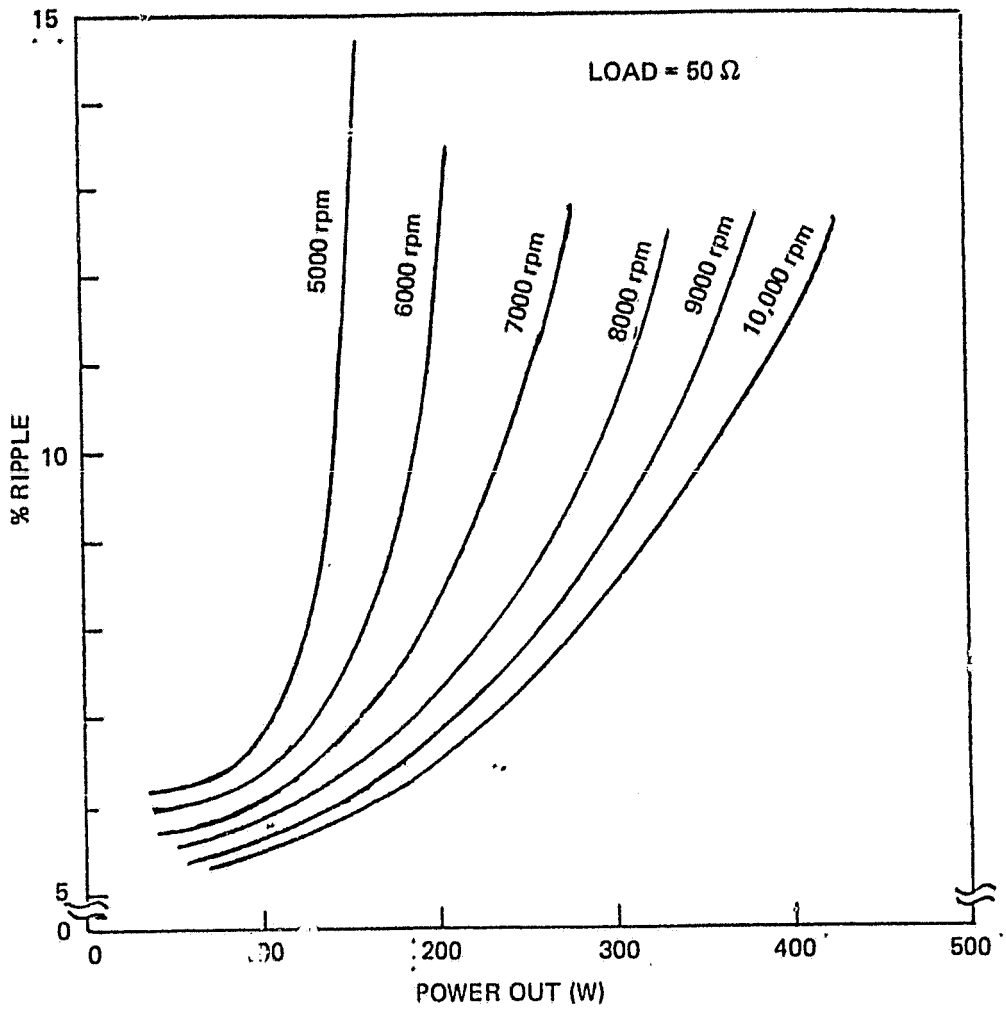

Figure 5.6. Generator Test. Output Ripple versus Output Power into a 50 Ohm Load with Speed as a Parameter

The losses are segregated into three components: mechanical, magnetic and electrical. Mechanical losses were shown in Figure 5.2. Electrical losses may be reduced by increasing the copper volume of the field windings as shown in Figure 5.7. As can be seen, the efficiency nears its asymptotic value when the winding volume is increased to 5 times the present volume.

Output winding losses may be reduced in a similar manner. For the particular motor design used, however, the output winding resistance was less than 2 ohms, and thus did not produce significant losses over the load range where significant power is produced.

The magnetic losses are intrinsic to the design, and represented by the asymptotic values of the curves in Figure 5.7. For example, at 10,000 rpm the asymptotic value is about 70%, giving intrinsic magnetic losses of about 30%.

5.3 MOTOR PERFORMANCE

Tests of motor performance (see Figure 5.8) were conducted as follows:

1. The inductor alternator rotor was brought to the desired speed by the DC motor.

2. A dual-phase function generator supplied two square waves, 90° out of phase and at the appropriate frequency, driving the input/output windings.

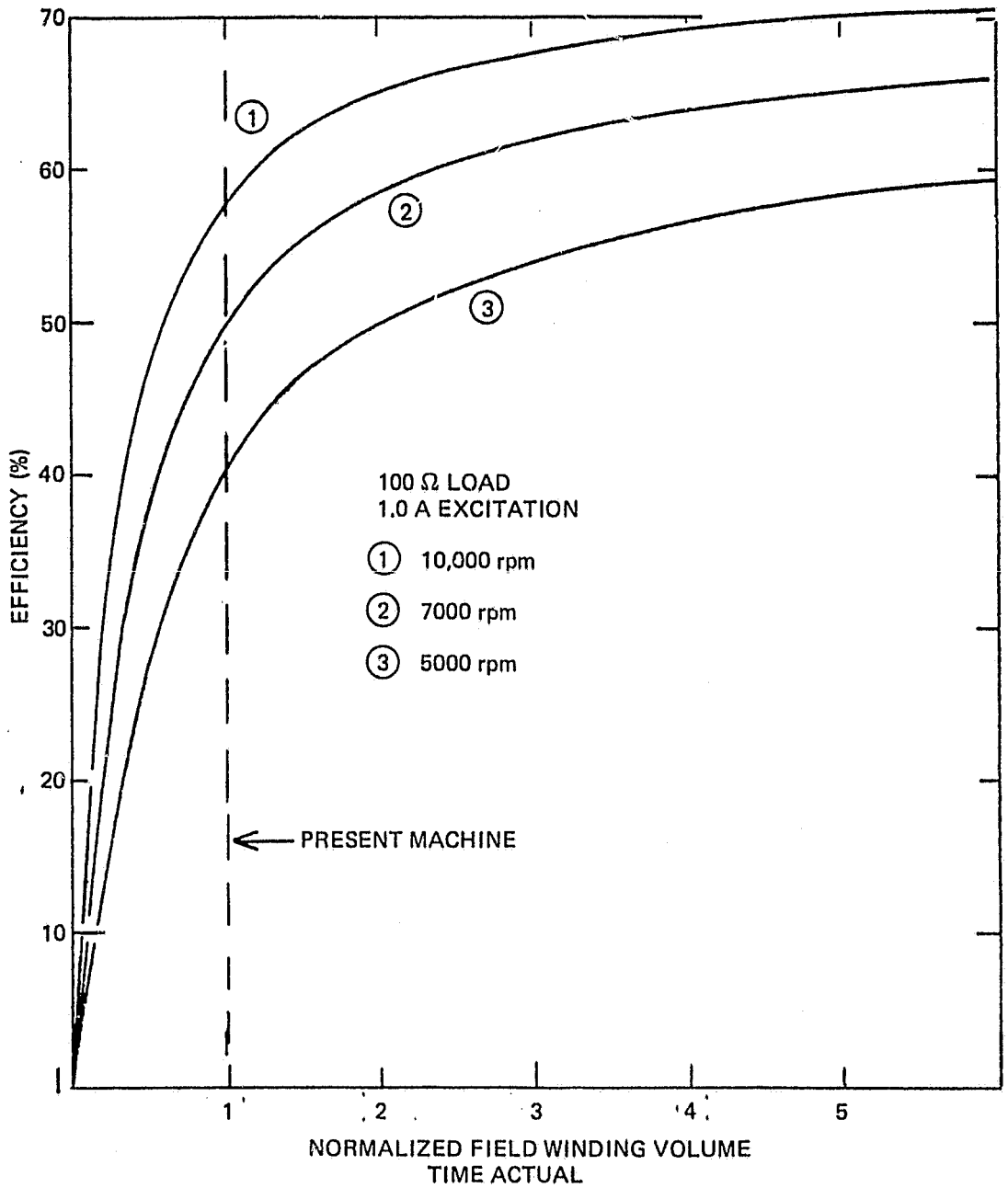

Figure 5.7. Efficiency (%) versus Normalized Field Winding Volume with Speed as a Parameter. Load = 100 Ohms, Excitation = 1.0 Ampere

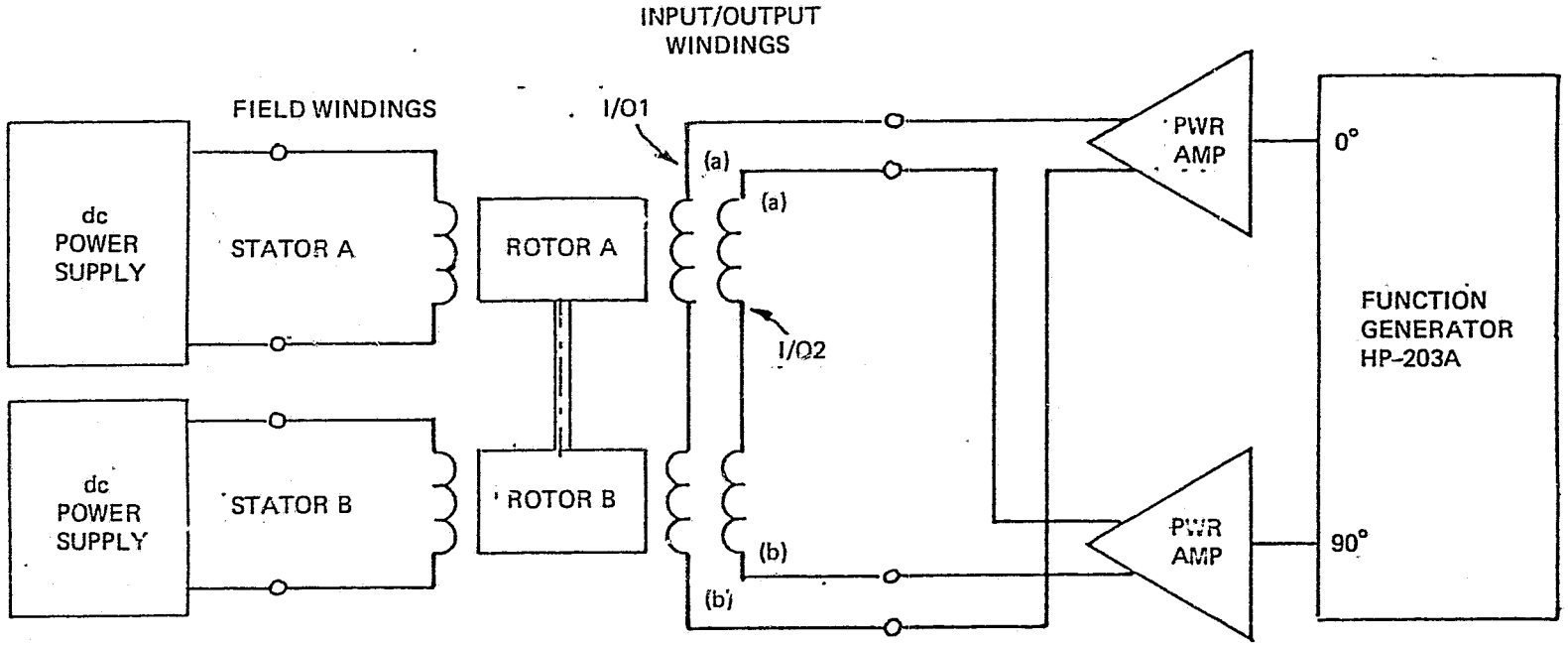

Figure 5.8. Motor Test Setup

3. The outputs of the function generator were amplified and applied to the inductor alternator input/output windings (Figure 5.9).

4. When field excitation was applied, the motor would tend toward the stable equilibrium point where mechanical and electrical frequencies were equal. In particular, once the two frequencies had been matched within approximately 5 Hz the rotor would "lock in" and oscillate about the equilibrium point, with typical settling time of 10 seconds.

5. The stable synchronous frequency described above is the frequency where no net electrical power flows into the inductor alternator. Net power flow was achieved by decreasing power into the DC motor while simultaneously tuning the B-field excitation.

6. At a given speed, maximum power transfer occurs at unstable equilibrium, since any attempt to draw more power causes the inductor alternator to drop out of synchronization. Measurements were made as close to this limit as was possible given the open loop control. Figures 5.9 (a) and (b) are typical of the waveforms obtained in this manner.

Net mechanical output power was found to be highly speed-dependent, as shown in Figure 5.10. At lower speeds, mechanical power output increases with

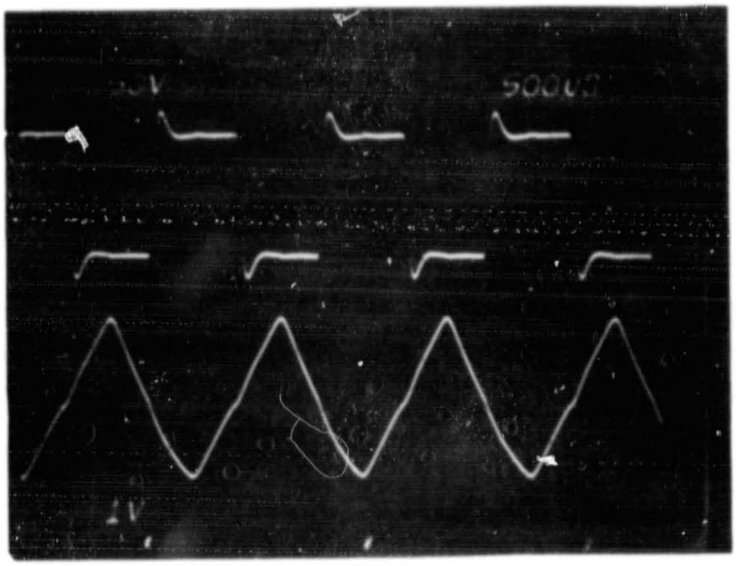

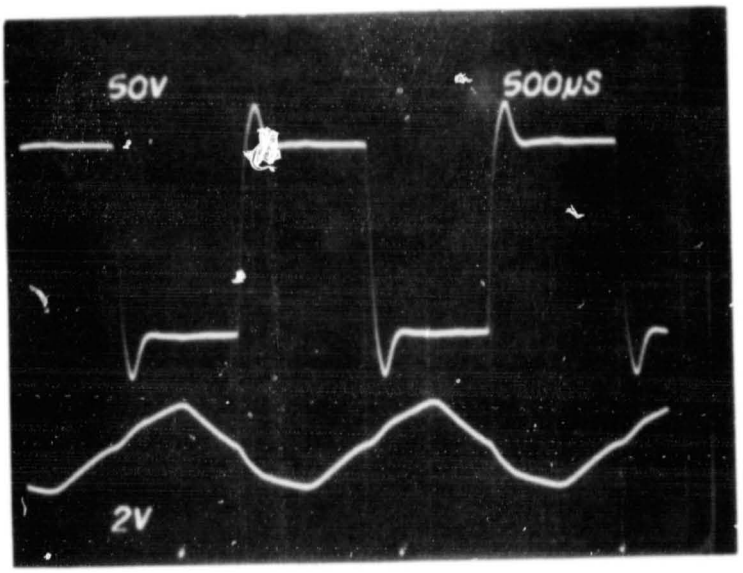

A) Motor Test. Input Voltage (top) and current (bottom); one phase. Power Input approximately 100 W

B) Motor Test. Input Voltage (top) and current (bottom); one phase. Power input approximately 200 W.

Figure 5.9. Motor Test Waveforms

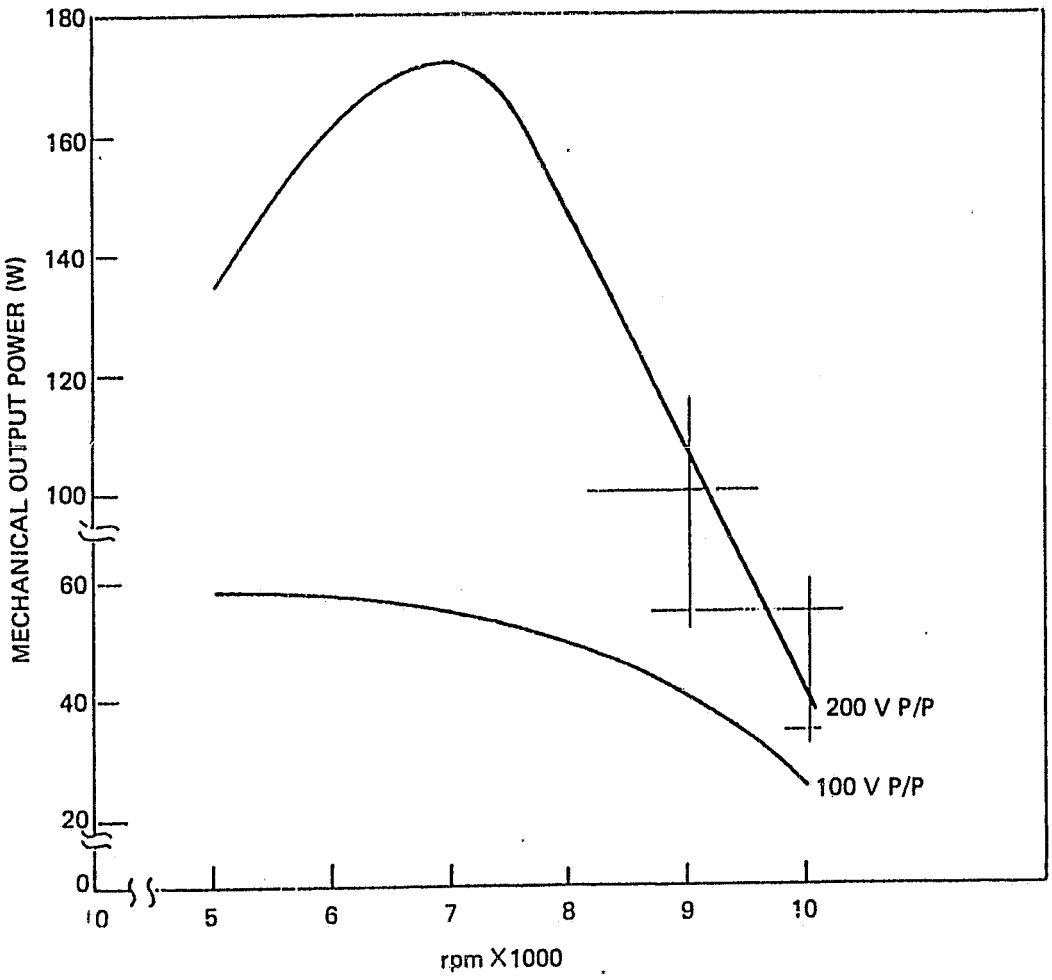

Figure 5.10. Motor Test. Net Mechanical Output Power versus Speed with ac Drive Voltages of 100 and 200 Volts Peak to Peak

increasing speed, as expected, but the magnetic losses shown in Figure 5.2 dominate at the higher speeds. This effect is also visible in the efficiencies plotted in Figure 5.11. Also note that while the higher 200V excitation produces more output power, it is at the cost of significantly greater magnetic losses, which manifest themselves as lower efficiencies.

5.4 DEMONSTRATION OF FREQUENCY CONVERSION

The inductor alternator was operated briefly as a frequency converter, with the A and B fields excited from a 60-Hz line. The inductor alternator was originally designed for this use (see Section 2.2). The test consisted of waveform measurements at various field excitations. Typical results are shown in Figures 5.12 (a) and (b) [2].

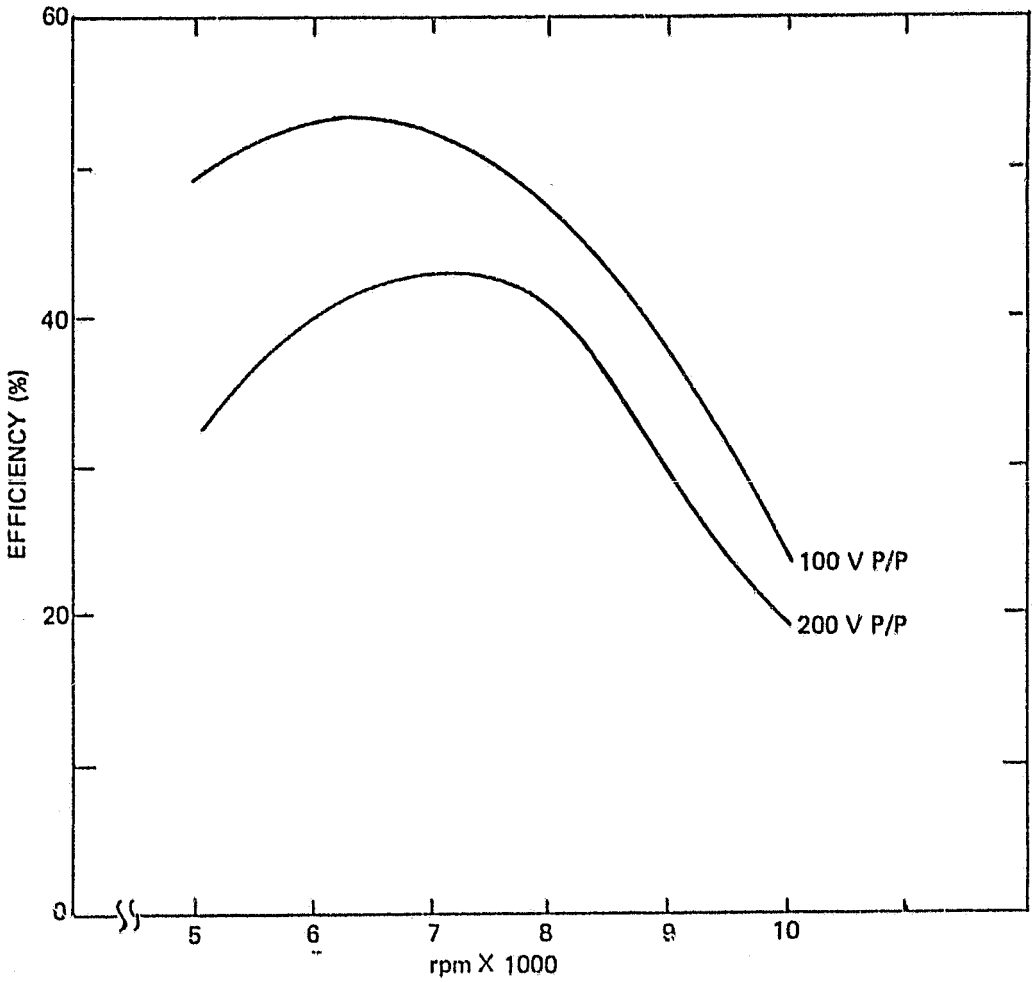

Figure 5.11. Motor Test. Efficiency versus Speed. ac Drive Voltages of 100 and 200 Volts Peak to Peak

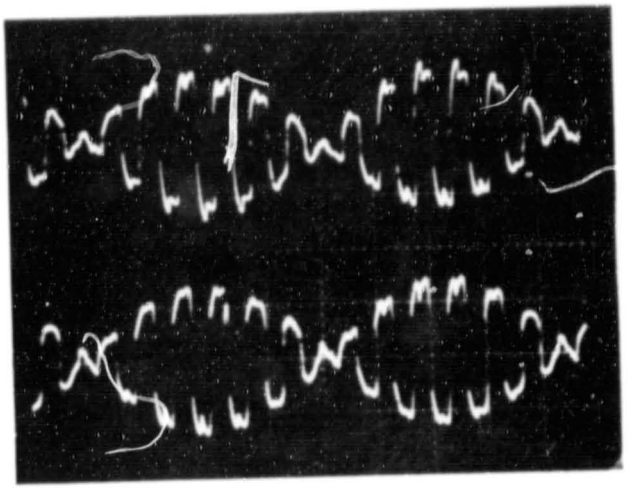

a. VOLTAGE OUTPUT FROM BOTH MACHINE PHASES DURING ac OPERATION INTO A 100 Ω RESISTIVE LOAD.

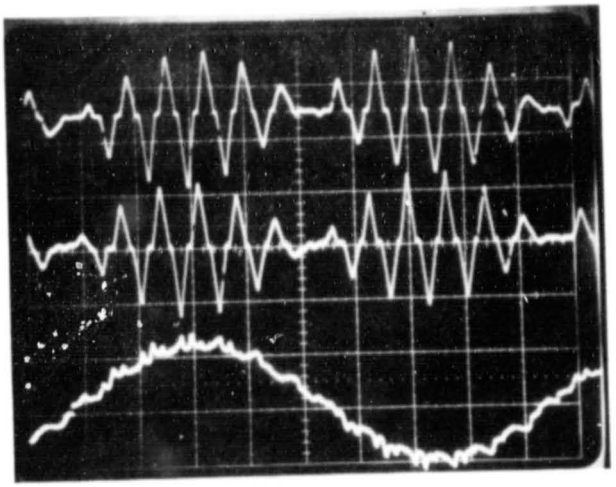

b. (TOP TWO TRACES) CURRENT OUTPUT OF BOTH MACHINE PHASES DURING ac OPERATION INTO A 100 Ω RESISTIVE LOAD.
(BOTTOM TRACE) CORRESPONDING LOAD VOLTAGE.

Figure 5.12. Field Modulation Demonstration. Voltage and Current Waveforms for Modulated (ac) Operation into a Real Load

6. CONCLUSIONS AND RECOMMENDATIONS

6.1 CONCLUSIONS

This project had as its goal the development of simple, low cost, and power conversion equipment. There were two principle objectives. The first objective was to demonstrate the performance of Draper Laboratory's dual field control concept and its potential for simplifying and reducing the cost of required power electronics in flywheel applications. The second objective was to demonstrate that this concept could be implemented with a specially designed inductor alternator. The dual field control concept was successfully implemented with an inductor alternator which was operated bidirectionally, a unique application of this type of machine. However, the concept could be implemented with any type of wound field synchronous machine. The inductor alternator appears to a good choice for those flywheel power conditioning applications where power density is not critical.

The most important aspect of dual field control is that the machine output may be phase shifted through the use of the field control so that current is in phase with terminal voltage and has harmonic content independent of load. There are two principle advantages in having current in phase with terminal voltage. First, the power stage can then be made with low cost naturally commutated thyristors. Second,low current ripple can be obtained without the use of heavy and expensive external filters. Thus the use of lower

cost power electronics is possible with dual field control as compared to other power converion techinques such as cycloconverters.

The control circuits were not tested experimentally, but by use of manual field controls it was demonstrated that, as predicted, the terminal voltage and current could be kept in phase over all operating conditions. Output ripple of approximately 6% can be achieved without filtering. If required, output ripple can be reduced further through input/output and field winding modification. The agreement between predicted waveforms and those measured in the inductor alternator is quite good. Deviation from predicted waveforms is due to the effects of resistance and saturation.

The specific power in the test machine is approximately 400 Watts per 35 lbs of material (11.4 W/lb). The test machine was deliberately designed using conservative techniques to facilitate analysis. The specific power could be increased by approximately a factor of 30 to approximately 300 W/lb in a high density design.

In the present design, machine losses are dominated by field and magnetic losses with efficiencies running in the 40-60% range. These efficiencies can be extended to 80% using the same stators at higher speeds and with additional input/output copper volume. In a new design power capabilities and efficiency can be traded against copper and air gap volumes. High

efficiency requires a large copper volume and small air gap whereas high specific power density requires large air gap and smaller copper volume.

6.2 RECOMMENDATIONS

The inductor alternator with dual field control has applications in areas where extreme ruggedness is required and design emphasis is not on power density. It also has application in areas where the rotor inertia could be utilized effectively, such as energy storage.

Follow-on work should be aimed at developing a complete dual field control system to demonstrate low cost and simplicity. If a dual field machine is used in an electric vehicle where weight is critical, an improved electromagnetic machine should be used. Development of a complete system including power stage, controls, and power converter at the 30 Hp (22 kW) level is recommended.

7. REFERENCES

1 Eisenhaure, D., G. Oberbeck, S. O'Dea and W. Stanton. Final Report on Research Toward Improved Flywheel Suspension and Energy Conservation Systems. Cambridge, MA: Charles Stark Draper Laboratory Report R-1108, November, 1977

2 Bliamptis, T. "A Field Modulated, Variable-Speed to Constant-Frequency Power Converter", Master's Thesis, Massachusetts Institute of Technology, Cambridge, MA, December 1980, also Charles Stark Draper Laboratory Report T-730